Preprints.org

Article

Aripiprazole, but Not Olanzapine, Alters the Response to Oxida-Tive Stress, Reducing the Activation of Mitogen-Activated Protein Kinases (MAPKs) and Promoting Cell Survival in FAO Cells

Barbara Kramar , Tinkara Pirc Marolt , Ayse Mine Yilmaz Goler , Dušan Šuput , Irina Milisav [*] , Maria Monsalve [*]

Article

Aripiprazole, but Not Olanzapine, Alters the Response to Oxidative Stress, Reducing the Activation of Mitogen-Activated Protein Kinases (MAPKs) and Promoting Cell Survival in Fao Cells

Barbara Kramar [1], Tinkara Pirc Marolt [1], Ayse Mine Yilmaz Goler [2,3], Dušan Šuput [1], Irina Milisav [1,4,*] and María Monsalve [5,*]

[1] University of Ljubljana, Faculty of Medicine, Institute of Pathophysiology, Zaloska 4, SI-1000 Ljubljana, Slovenia; barbara.kramar@mf.uni-lj.si (B.K.); tinkara.pircmarolt@mf.uni-lj.si (T.P.M.); dusan.suput@mf.uni-lj.si (D.Š.)

[2] Marmara University, Genetic and Metabolic Diseases Research and Investigation Center, Istanbul, Turkey; ayse.mine@marmara.edu.tr

[3] Marmara University, School of Medicine, Department of Biochemistry, Istanbul, Turkey

[4] University of Ljubljana, Faculty of Health Sciences, Laboratory of Oxidative Stress Research, Zdravstvena pot 5, SI-1000 Ljubljana, Slovenia

[5] Instituto de Investigaciones Biomédicas Sols-Morreale (CSIC-UAM), Arturo Duperier, 4, 28029-Madrid, Spain

* Correspondence: irina.milisav@mf.uni-lj.si (I.M.); mpmonsalve@iib.uam.es (M.M.)

Abstract: Chronic administration of atypical antipsychotics (AAPs) is commonly associated with increased cardiovascular disease load. Although the increase in weight gain and related disease risk is generally considered the main contributing factor, direct interference with mitochondrial bioenergetics, particularly in the liver, where these drugs are catabolized, is emerging as an additional relevant contributor to metabolic disease risk that needs to be considered. In this study, we compared the effects of two AAPs with disparate metabolic profiles, olanzapine (OLA), which is obesogenic, and aripiprazole (ARI), which is not, on the response of Fao cells to oxidative stress. We found that Fao cells treated with ARI survive better a challenge with H_2O_2 while OLA treatment has the opposite effect. This enhanced survival is not related to a reduction in the apoptosis rate. In fact, ARI treated cells display higher apoptotic rates than control cells exposed to H_2O_2. Gene expression analysis of pro and anti-apoptotic factors revealed that the changes induced by H_2O_2 were generally dampened in ARI treated cells, but not in OLA treated cells, suggesting a reduced responsiveness to stimuli, a notion that was consistent with a reduced activation of MAPK and STAT3 phosphorylation in response to H_2O_2, while OLA enhanced their activation in response to H_2O_2. Loss of stress response in ARI treated cells is consistent with the elevation of mitochondrial production of $O_2^{\bullet-}$, a known desensitizing factor. The physiological relevance of the increased production of $O_2^{\bullet-}$ in ARI treated cells is further supported by the observed elevation of the mitophagy flux in ARI treated cells, likely related to mitochondrial damage. An additional relevant finding was that OLA treatment protected the proteasome activity in Fao cells exposed to H_2O_2, an effect possibly related to the better preservation of stress signaling and mitochondrial function in OLA treated cells. In sum, this study highlights the underlying alterations in cell physiology derived from the interference of ARI with mitochondrial function, that de-sensitize cells to stress signaling, while OLA has the opposite effect.

Keywords: atypical antipsychotics (AAPs); secondary drug effects; schizophrenia; liver; mitochondria; oxidative stress (OS); MAPK

1. Introduction

Atypical antipsychotics (AAPs) are the first line of treatment for schizophrenia but are also commonly prescribed for the treatment of other psychiatric disorders, including bipolar disorder and

treatment-resistant depression, as well as for the management of community-dwelling persons with Alzheimer's disease, other forms of dementia [1], behavior issues associated with autism and intellectual disability [2] and other behavior-mood disorders including attention-deficit/hyperactivity disorder (ADHD) [3]. The global prevalence of antipsychotic use in adults has been estimated at 1-2%, reported at 1.7 % in the USA in 2020 [4], with fast-increasing rates in children and adolescents [5]. AAPs are weak dopamine D2 receptor blockers with variable additional pharmacological targets that commonly involve serotonin (5-HT) receptors [6]. The ratio of 5-HT2A/D2 and 5-HT2C/D2 receptor affinity and a rapid dissociation constant from the D2 receptor are two important factors that distinguish AAPs in terms of efficacy and side effects [7]. Other molecular targets additionally characterize the receptor profile of AAPs: 5-HT1 partial agonism, H1 antagonism, α2 antagonism, muscarinic antagonism and positive allosterism, brain-derived neurotrophic factor (BDNF) production, and blockade of glycine transporter (GlyT) [8].

Since AAPs prescriptions are generally life-long, handling side-effects is a relevant concern for physicians and patients [9]. Although some of these are related to their direct pharmacology targets in the CNS, they are frequently drug-specific and thus likely related to off-target effects or derived from their chemical structures that differentially interfere with cellular physiology.

The most common side-effects are metabolic complications such as dyslipidemia [10], and impaired glucose homeostasis [11]. These occur frequently, but not always, along with significant weight gain [12], and always lead to a relevant increase in cardiovascular disease (CVD) risk [13]. The fact that the affected groups tend to have, even before treatment starts, a higher prevalence of metabolic syndrome (MetS) and higher CVD risk than the general population further highlights the relevance of the problem [14].

The mechanisms involved have been extensively investigated but have yet to be clarified. Although some risk derives from the patients themselves, the increased CVD risk is still mainly associated with the treatment [15]. It has been proposed that the sedative effect of some AAPs and the related increased food intake play a fundamental role [16]. However, other factors can contribute. AAPs cause hepatotoxicity and inflammation in the liver [17]. Since the liver is a central metabolic organ, this has an essential impact on the systemic metabolic homeostasis [18]. The mechanisms involved in liver toxicity are generally regarded as related to AAPs catabolism. AAPs are xenobiotics whose catabolism involves P450 enzymes, leading to enhanced productions of reactive oxygen species (ROS) and, in some cases, the accumulation of reactive intermediate metabolites [19]. More recently, some studies have investigated the possible role of mitochondria as an alternative source of elevated ROS levels following AAPs administration [20]. The high hydrophobicity of these molecules can lead to their accumulation in biological membranes, including the mitochondrial inner membrane (IMM), and thus alter cell signaling and bioenergetics; in fact several AAPs have been found to directly alter mitochondrial bioenergetics [21]. Importantly, mitochondrial damage and oxidative stress have also been shown to play a negative role in neurodegenerative, neurodevelopmental, and behavior disorders [22]. Furthermore, recent studies suggest that reduced mitochondrial homeostasis, that is, the impairment of mitochondria regulation in terms of activity and turnover, has a negative impact on the cellular capacity to respond to stressors and thus hampers the cellular capacity to prevent the accumulation of cellular damage [23] and may also dysregulate the activation of cell death related pathways. An early response to mitotoxins is the induction of mitochondrial fission that can enable the elimination of damaged mitochondria through mitophagy [24]. Fission has been shown to reduce both the mitochondrial oxidative capacity and its sensitivity to mitochondrial-dependent cellular apoptosis, a process that is particularly relevant in the cancer [25]. In sum, interference with mitochondrial function has been shown to fundamentally alter cell physiology, the cellular capacity to adequately respond to nutrient availability and oxidative stress [26], to increase metabolic and cardiovascular risk [27] and to have a negative impact on neurological homeostasis [24]. Therefore, to minimize the negative side effects of AAPs administration, it is of fundamental importance to evaluate their particular cellular effects and the mechanisms involved.

Clozapine and olanzapine (OLA) are the worst AAPs in terms of increased MetS risk [28]. OLA is the 4th most commonly prescribed AAP, accounting for about 10% of the total AAPs prescriptions.

Importantly, type 2 diabetes (T2D) is not strictly correlated with adiposity. In fact, 25 % of patients develop hyperglycemia without gaining weight and this metabolic alteration can happen in the early period of the treatment and precede weight gain. Nevertheless, it is important to highlight that weight gain undoubtedly represents an aggravating factor [29]. On the other hand, OLA reduces both positive and negative psychotic symptoms significantly more than most other AAPs and is associated with a significant reduction of depressive episodes and a more significant improvement in the social functioning [30]. Therefore, it is one of the most commonly prescribed AAPs [31].

The precise mechanism of OLA action is unknown since it exhibits a wide array of receptor affinities that may explain the clinical and adverse effects. Efficacy in schizophrenia may be by a combination of dopamine D2 and serotonin 5-HT2A receptor antagonism in the mesolimbic pathway [32]. OLA shows a higher affinity for serotonin 5-HT 2A receptors than dopamine D2 receptors with selectivity for dopamine receptor subtypes in the mesolimbic and mesocortical systems over the nigrostriatal and tuberoinfundibular systems; perhaps the reason for the reduced risk of extrapyramidal side effects and hyperprolactinemia. Antagonism at muscarinic, histaminic, and alpha-adrenergic receptors leads to side effects, such as dry mouth, micturition difficulty, constipation, weight gain, somnolence, dizziness, and hypotension [33]. OLA is well absorbed when taken orally with 80 % bioavailability although undergoing first-pass metabolism, and reaches peak plasma concentrations after 6 h where it is predominantly bound to albumin (90 %) and α1-acid glycoprotein (77 %). It has linear kinetics with an elimination half-life of 21–54 h reaching steady-state concentration after one week [34]. In the liver, OLA is metabolized to its 10- and 4'- N-glucuronides, 4'-N-desmethyl olanzapine [cytochrome P450(CYP) 1A2] and olanzapine N-oxide [flavin monooxygenase 3], and then cleared. Metabolism to 2-hydroxymethyl olanzapine via CYP2D6 is a minor pathway. Furthermore, OLA does not inhibit CYP isozymes [7]. However, OLA has been shown to increase plasma transaminases levels, suggesting drug-induced liver damage, liver steatosis, and even non-alcoholic fatty liver disease (a pathological development of simple liver steatosis) in some cases, the effects that could be related to its impact on whole-body metabolism [35]. Some *in vitro* studies have evaluated the effect of OLA on the mitochondria and its impact on redox homeostasis. For example, OLA has been shown to induce mitochondrial fission [36], the down-regulation of electron transport chain (ETC) genes as well as to decrease mitochondrial enzyme activity, ATP synthesis, and oxygen consumption rate (OCR) in circulating leukocytes of patients at elevated risk for MetS [37]. Furthermore, increased oxidative stress and glutathione depletion was detected in hepatocytes treated with OLA in one study, and implicated both mitochondrial toxicity and CYP450 activity [38]. Other studies on the mitochondrial toxicity of AAPs imply that OLA has very little or no direct mitochondrial toxicity, while other AAPs, and in particular, aripiprazole (ARI), have been shown to reduce mitochondrial OCR [39] in liver cells, an effect that may be related to the inhibition of ETC Complex I (CI) or CV activity [40]. Although a clear picture of AAPs interference on mitochondria has not emerged yet, available data suggest that it may trigger mitochondrial dysfunction and lead to the development of MetS.

ARI is the 2nd most widely prescribed AAP, accounting for about 20 % of the total number of AAPs prescriptions. It is a partial agonist of D2 receptors [41], a partial 5-HT1A receptor agonist, and a 5-HT2A receptor antagonist. Its unique pharmacological properties compared to other AAPs, along with the resulting lack of the sedative and hyperphagic effects, have prompted physicians to recommend its prescription in patients at risk of or with MetS. ARI has been shown to induce debilitating extrapyramidal syndromes (EPS) in ~ 5 to 15 % of patients likely due to off-target effects. ARI is catabolized in the liver by N-dealkylation, hydroxylation, and dehydrogenation by the cytochrome P450 (CYP)3A4 and 2D6 enzymes, thus polymorphisms in these genes can reduce drug tolerance [42][43]. However, LiverTox NIH publication notes, updated in 2023 indicates that ARI's hepatotoxicity likelihood score falls under the D category, namely, possible rare cause of clinically apparent liver injury [44]. Nevertheless, a literature search reveals that several cases related to ARI-induced liver injury have been reported [45] but, there are no large-scale epidemiological studies to provide sufficient pharmacoepidemiology evidence [46]. Of note, chronic feeding of adult *Drosophila melanogaster* with ARI has been shown to result in structural damage of brain and thoracic muscle

mitochondria, along with locomotor dysfunction [47], supporting the notion that ARI mitotoxicity occurs *in vivo* and can have a significant pathologic role.

In order to shed some light on the mechanisms involved in ARI and OLA secondary effects, we used Fao cells, a rat hepatocarcinoma (HCC) cell line with well-preserved metabolic plasticity and ROS sensing and tested how ARI and OLA 24 h single treatment, as well as daily treatments for several weeks, modified the cellular response to an oxidative challenge. Our results imply that ARI mitotoxicity reduces the cellular sensitivity to MAPK activation and as a result show reduced cell death rates following an oxidative challenge.

2. Materials and Methods

Reagents were purchased from Sigma-Aldrich (Merck, Darmstadt, Germany) unless otherwise indicated.

Cell culture. The rat hepatoma cell line Fao (#89042701, ECACC) was grown at 37 °C in a humidified atmosphere with 5 % CO_2, in Coon's F-12 Modified Liquid Medium (#MBC-F0855) supplemented with 10 % fetal bovine serum (#10270-106, Gibco, Thermo Fisher Scientific, Whaltham, MA, USA), 1 % penicillin/streptomycin (#15140-122, Gibco, Thermo Fisher Scientific, Whaltham, MA, USA) and 1 % GlutaMAX supplement (#35050038, Gibco, Thermo Fisher Scientific, Whaltham, MA, USA). Cells were seeded on 96-well flat-bottom cell culture plate (40.000 cells/well) for cytotoxicity assessments, Collagen coated (5 µg/cm²) 1 cm² glass cover slips positioned on 24-well plates (200.000 cells/well) for MitoSOX assessment, 12-well cell culture plates (500.000 cells/well) for caspase activity determination, 6-well cell culture plates (1 million cells/well) for proteasomal activity measurement, 6-well cell culture plates (1 million cells/well) and T25 flasks (3 million cells/flask) for gene and protein expression analyses. To test ARI and OLA effects Fao cells were grown in the presence of a control vehicle, 0.12 % DMSO (#67-68-5, Acros Organics, Thermo Fisher Scientific, Whaltham, MA, USA), ARI (#PHR1784) or OLA (#PHR1825) at doses corresponding to laboratory alert levels in patients' sera (2.23 µM ARI and 0.32 µM OLA) and at 6µM ARI/OLA. Different batches of cells were tested in parallel. Cells were exposed to ARI/OLA for 24 h (single treatment) or 4-8 weeks (repeated treatment), with media changes every 24 h, prior to being challenged with 1.5/3 mM H_2O_2 for 3 h and harvested.

MitoSOX. Cells were seeded on Collagen-coated glass coverslip glasses 24 h prior to treatment. Following treatment, cells were washed with 1x PBS and labeled with 3 µM MitoSOX in HBSS (1.26 mM $CaCl_2$, 0.49 mM $MgCl_2 × 6H_2O$, 0.41 mM $MgSO_4 × 7H_2O$, 5.33 mM KCl, 0.44 mM KH_2PO_4, 4.17 mM $NaHCO_3$, 137.93 mM NaCl, 0.34 mM Na_2HPO_4, 5.56 mM D-glucose) in the darkness for 10 min at 37 °C. Then, the cells were washed with 1x PBS, fixed with 4 % paraformaldehyde for 15 min at room temperature, washed again with 1x PBS and stored at 4 °C 1x PBS in the darkness prior to mounting on slides with ProLong Diamond Antifade Mountant (Thermo Fisher Scientific, USA). Slides were stored in the dark at 4 °C. Images were captured using a fluorescence inverted microscope (Olympus IX81F, Olympus Corporation, Japan). The images' scale bar is 50 µm.

Cell viability. Cytotoxicity was evaluated using 0.04 mg/mL Neutral Red (NR, 3-Amino-7-dimethylamino- 2-methylphenazine hydrochloride; N4638) staining as previously described [48]. NR assay was performed for single ARI/OLA treatments. Dehydrogenase activity was determined using the Thiazolyl Blue Tetrazolium Bromide assay (MTT, #M5655). The extracellular release of lactate dehydrogenase (LDH) was measured using the LDH Cytotoxicity Detection Kit (#MK401, Takara Bio Europe, Saint-Germain-en-Laye, France) as previously described [49]. Cells' images were captured using an inverted microscope (Leica, Wetzlar, Germany). Representative images are included in Supplementary Figure S1. The images scale bar is 50 µm.

Caspase activity. Caspase 3/7 and 9 activities were assessed using Caspase-Glo reagents (#G810C, (#G811C #G816C, #G822C, Promega, Madison, WI, USA) following the manufacture's instructions. Caspase cleavage releases an active luciferase substrate whose luminescence signal is proportional to caspase activity and is detectable in a Luminometer. This assay was used following ARI and OLA treatments with and without the 3 h H_2O_2 challenge, as well as with cells treated for 3 h with 1 µM staurosporine (STS), a powerful inductor of apoptosis through the mitochondrial pathway, prior to

harvesting. The cells were washed with 1x PBS and stored at –80 °C. Cells were next lysed in CCLR lysis buffer (# E1531, Promega, Madison, WI, USA), centrifuged and the supernatant was saved, diluted with CCLR and Caspase-Glo 9 or Caspase-Glo 3/7 reagent were added. Following 20 min incubation, the luminescence signal was captured with a luminometer 20/20n (Turner Biosystems Corp., Promega, Madison, WI, USA). Protein concentration in the extract was determined using the Pierce 660 nm Protein Assay Reagent (Thermo Fisher Scientific, USA) and used to determine the luminescence/µg of protein in the sample.

mRNA analysis. Total RNA was isolated and retro-transcribed as previously described [48]. Gene expression was assessed by qPCR analysis using TaqMan probes in a 7500 Real-Time PCR System using the SDS v1.3.1 software (Applied Biosystems, Thermo Fisher Scientific, Waltham, MA, USA). Genes expression was calculated relative to the expression of the reference gene, 18S rRNA (#Rn18s) using the equation: target/reference=(E(reference)Ct(reference))/(E(target)Ct(target)). Biological replicate values were then divided by the average of all samples in the replicate to account for multi-plate experiments variability and expressed as logarithmic fold change normalized to the baseline sample without a probe. The following TaqMan probes labelled with the FAM dye (Thermo Fisher Scientific, Whaltham, MA, USA) were used: the reference gene Rn18s (#Rn03928990_g1), *Cas3* (#Rn00563902_m1), *Cas9* (#Rn00581212_m1), *p38* (#Rn00578842_m1), *Stat3* (#Rn00680715_m1), *Bax* (#Rn01509178_m1), *Bcl2* (#Rn99999125_m1), *BclXL* (#Rn00437783_m1), *Mcl1* (#Rn00821024_g1), *Bid* (#Rn01459517_m1), *Diablo* (#Rn01480487_g1).

Protein extraction and western blotting (WB). Whole-cell lysates were obtained as described [50]. In brief, 20 µg of whole protein extracts, were loaded onto 10 % and 12 % acrylamide gels to be separated by standard sodium dodecyl sulfate-polyacrylamide gel electrophoresis (SDS-PAGE). The gel was stained with Coomassie blue (#27813Fluka,) to control for equal loading and proteins were transferred onto PVDF Immobilon-P membranes (#IPVH00010) using a semi-dry transfer system (BioRad Hercules, CA, USA). Membranes blocked with 3 % BSA in TBS-T were incubated overnight at 4 °C with primary antibodies washed with TBS-T and then incubated with horse radish peroxidase-conjugated goat anti-rabbit or goat anti-mouse secondary antibodies (BioRad Hercules, CA, USA #1706515 and #1706516, respectively) washed again and developed with Clarity ECL Substrate (BioRad Hercules, CA, USA). The luminescence signal was captured on X-ray films (AGFA, CP-BU, 0413) and developed by Curix60, 9462 developing machine then quantified using the v.5.2.5. Image Studio software (LI-COR, Lincoln, NE, USA). Experiment's replicates on separate membranes were normalized calculating the ratio of individual values by the average signal for all samples in the membrane. Primary antibodies used were, from Cell Signaling Technology (Danvers, MA, USA): Phospho-p38 MAPK (Thr180/Tyr182) (#9211), p38 MAPK (#9212), Phospho-SAPK/JNK (Thr183/Tyr185) (#9251), SAPK/JNK (#9252), Phospho-p44/42 MAPK (Erk1/2) (Thr202/Tyr204) (#9101), p44/42 MAPK (Erk1/2) (#9102), Phospho-Stat3 (Tyr705) (D3A7) XP Rabbit mAb (#9145), Stat3 (D3Z2G) Rabbit mAb (#12640), from Abcam (Cambridge, UK): Bcl-xL (#2762), LC3B (#2775) and from BD transduction Laboratories (Franklin Lakes, NJ, USA): Tim23 (#611222). Raw data is included in Supplementary Figures S2 and S3.

Proteasome activity was determined as previously described [51], a procedure is based on 7-Methoxycoumarin-4-acetic acid (MCA) fluorescence, which is released following cleavage of the fluorogenic peptide suc-LLVY-MCA in the presence of chymotrypsin-like proteasome activity. The method allows the separate determination of the 20S and the 26S proteasome activities by using its differential requirement for ATP. The 20S subunit does not require ATP, while it is necessary for the proteolytic activity of the fully assembled 26S proteasome. In brief. Following treatments, cell culture plates were washed with 1x PBS and stored at -80 °C. Following thawing, cells were scraped with a rubber spatula in proteasome assay (PA) lysis buffer (250 mM sucrose, 30 mM HEPES, 20 mM $MgCl_2$, 1.3 mM EDTA, 1.6 mM DTT, pH 7.8), homogenized using a 0.5 mm sonotrode (UP50H, Hielscher, Germany), in sets of three, with 10 0.5 s pulses at 80 % amplitude and then centrifuged. The supernatants were stored at -80 °C. Following thawing, 10 µl of the sample was placed on black 96-well plates along with the reaction mixture corresponding to the proteasome to be analyzed (20S: 1.8 ⌀M DTT, 16 mM deoxyglucose, 0.1 mg/mL hexokinase in PA; 26S: 1.8 ⌀M DTT 4.5 mM ATP in PA).

The reaction was activated by the addition of 180 μM substrate suc-LLVY-MCA and following 1 h incubation at 37 °C the fluorescence was measured in a Victor3 reader, excitation 355 nm, emission 460 nm (PerkinElmer, Waltham, MA, USA). Proteasome activity was estimated as the amount of MCA released per time unit per μg of protein, predetermined with the Pierce 660 nm Protein Assay Reagent (Thermo Fisher Scientific, Waltham, MA, USA).

Statistical analysis was performed with GraphPad Prism 10.1.1 using its inbuilt algorithm to test the equality of variances from medians with the Brown-Forsythe test. One-way ANOVA was used in case of equal variances, followed by the Dunnett's multiple-comparisons test (when testing multiple experimental groups against a single control group) or Tukey's multiple-comparison test (when studying a relationship between variables). Unpaired *t* test was used when comparing two samples (LC3B data). Two-way ANOVA was used on two sets of data, how two independent variables, in combination, affect a dependent variable. In particular, it was used to test for the interaction of the phosphorylated and non-phosphorylated forms of the proteins JNK and ERK derived from western blot analysis. Data from statistical tests (Brown-Forsythe, One- and Two-way ANOVA, t-test) were compiled and are included in Supplementary Tables S1–S5. Treated samples were compared to the baseline and untreated controls. All data are presented as mean ± standard deviation (SD), and the significance level was set at $p<0.05$. Statistical parameters, sample sizes (n) and p-values, are noted in the figure legends.

3. Results

Mitochondrial superoxide ($O_2^{\bullet-}$). In order to investigate the effects of ARI and OLA interference with mitochondrial function, we first determined mitochondrial $O_2^{\bullet-}$ production using MitoSOX staining in ARI- and OLA-treated Fao cells and found that at a concentration of 6 ⍟M, a single ARI but not OLA treatment, produced a significant increase in mitochondrial $O_2^{\bullet-}$ (Figure 1a). This implies that ARI had significant mitochondrial toxicity, a result consistent with the previous observation that ARI at this dosage and timing reduced mitochondrial OCR and increased cellular H_2O_2 levels [39].
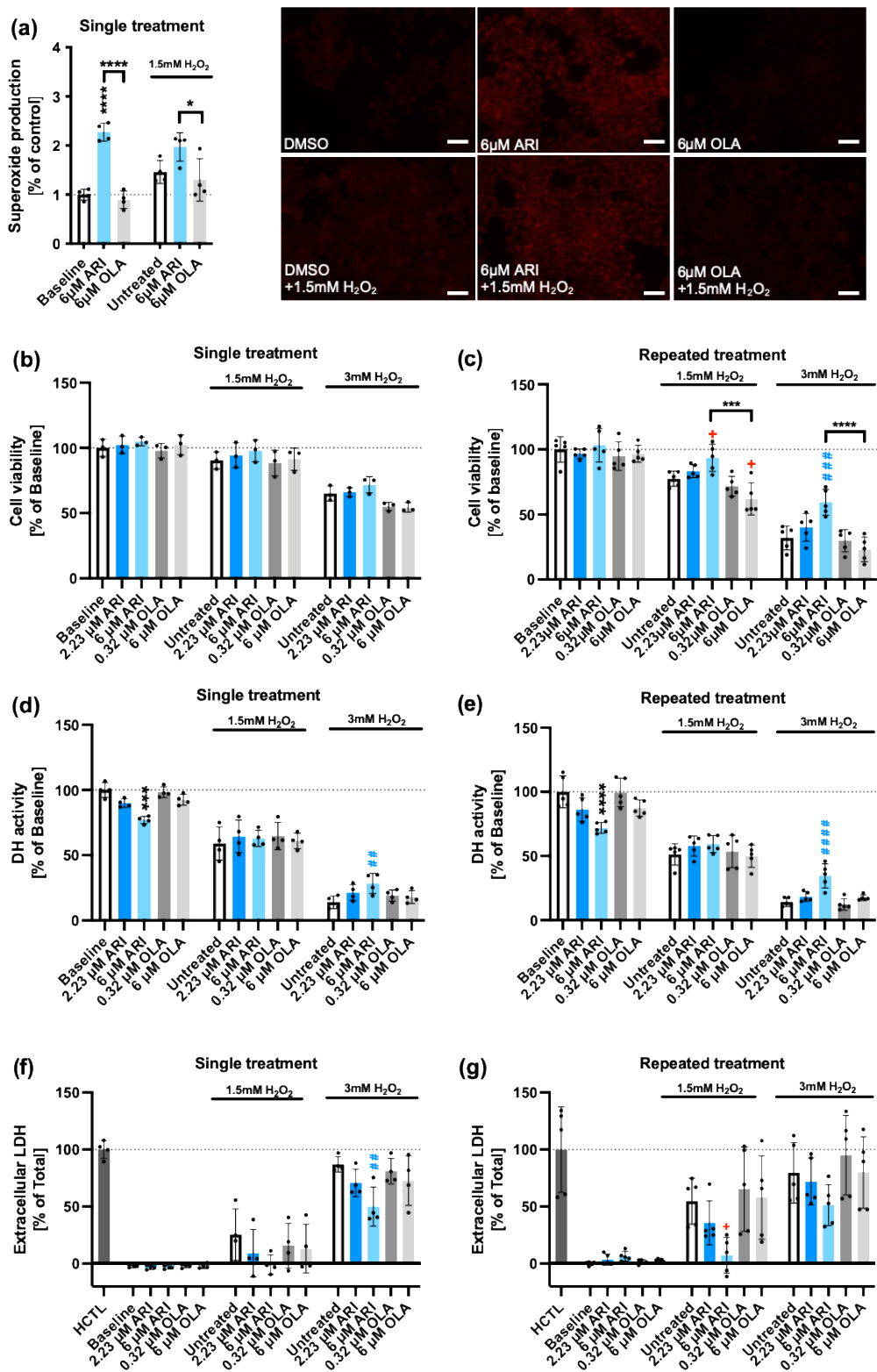
Figure 1. *Superoxide production and cell viability.* (**a**) Treated Fao cells were stained with MitoSOX assay to evaluate mitochondrial $O_2^{\bullet-}$ levels. Cell viability was tested by neutral red (NR) accumulation (**b, c**), dehydrogenase (DH) activity by MTT (**d, e**) and extracellular lactate dehydrogenase (LDH) by LDH release (**f, g**) assays. Graphs (**b**),(**d**) and (**f**) represent data from single (24 h) ARI/OLA treatments and graphs (c), (e) and (g) from repeated treatments. NR, MTT and LDH assays' baseline data (no H_2O_2 added) for both single and repeated treatments (b-g) are re-used under CC-BY4.0 license [49], as well as the NR assay results with 1.5 and 3 mM H_2O_2 in repeatedly treated cells (**c**) [48]. The graphs show mean ± standard deviation (SD) values analyzed by one-way ANOVA followed by Dunnett's test. Baseline ARI/OLA samples were compared to baseline control without H_2O_2 (*), 1.5 mM H_2O_2

ARI/OLA treated cells were compared to 1.5mM H_2O_2 untreated controls (+) and 3 mM H_2O_2 ARI/OLA treated samples were compared to 3 mM H_2O_2 untreated controls (#). Tukey's test was used to compare 6 μM ARI with 6 μM OLA samples (*above the line indicating the comparison). */+$p \leq 0.05$, ##$p \leq 0.01$,**/###$p \leq 0.001$, ****/####$p \leq 0.0001$. (a): $n = 4$; (b, e): $n = 3$; (c, d): $n = 4$; (f, g): $n = 5$. HCTL: "high control", maximal release of LDH.

ROS generally induce compensatory responses, including enhanced expression of antioxidants. However, previous observations implied that in single treatments Fao cells did not increase antioxidant capacity since at least superoxide dismutase (SOD), glutathione peroxidase (GPx) and catalase activities were not significantly modified in response to ARI, however, the activities of GPx and catalase significantly increased over the control upon continuous exposure to 6 μM ARI for 4-8 weeks [39]. In sum, increased ROS production was not linked to an overall increase in antioxidant capacity following a single treatment, but may do so following a long-term exposure, suggesting that long-term ARI treatment could be modifying the cellular capacity to respond to oxidative stress.

To evaluate this possibility, the response of Fao cells was tested following repeated exposure to ARI/OLA for 4-8 weeks, to an oxidative 3 h challenge with 1.5-3 mM H_2O_2. It was found that 6 μM treated ARI cells significantly increased the activity of two antioxidants, SOD and catalase, the protein levels of the antioxidant heme oxygenase-1 (HO-1), as well as, upregulated the gene expression of sulfiredoxin-1 (*Srxn1*), another antioxidant, and *Foxo3a*, a transcription factor that controls antioxidant gene expression. In contrast, 6 μM OLA did not induce any of these changes [48], implying that ARI but not OLA significantly enhanced resistance to oxidative stress upon oxidative challenge. Consistently, repeated exposure to 6 μM ARI was shown to reduce Fao cell death induced by 1.5 mM and 3 mM H_2O_2, while OLA had the opposite effect [48].

In order to determine if ARI elicited changes in the response to an oxidative challenge required a long-term adaptation (repeated treatment), we tested how and if a single treatment with ARI/OLA modified the response of Fao cells to an oxidative challenge with 1.5-3 mM H_2O_2. Therefore, we evaluated mitochondrial $O_2^{\bullet-}$ levels, using MitoSOX staining, in Fao cells treated with 6 ◎M ARI/OLA followed by 3 h exposure to 1.5 mM H_2O_2. We found that ARI-treated cells had significantly higher levels of $O_2^{\bullet-}$ than OLA-treated cells, while $O_2^{\bullet-}$ production in OLA-treated cells did not differ from controls, a result similar to that obtained in the presence of 1.5 mM H_2O_2 (Figure 1a).

Cellular viability. Next, we aimed to determine if these differences impacted the cellular viability of ARI-/OLA- pretreated cells challenged with 1.5-3 mM H_2O_2 for the last 3 h. First, we tested the lysosomal uptake of the neutral red (NR) dye, to identify living cells. In single-treated cells, 3 mM H_2O_2 significantly decreased cell viability, but we did not find significant differences among the treatment groups (Figure 1b). However, we previously observed [48] that in repeated treatments, at both 1.5 and 3 mM H_2O_2, which decreased cell viability in non-treated cells, 6 μM ARI treated cells had significantly higher NR levels than non-treated controls, while following the 1.5 mM H_2O_2 challenge, 6 μM OLA treated cells survived significantly less than non-treated controls (Figure 1c). These results imply that ARI-treated cells, although enduring higher ROS levels, are more resistant to oxidative stress-induced cell death. We further tested this concept using an alternative viability test, MTT, which measures cellular NAD(P)H dehydrogenase (DH) activities and is, therefore, also indicative of the cellular metabolic status. In non-treated controls both 1.5 and 3 mM H_2O_2 significantly reduced DH activity. For cells exposed to 1.5 mM H_2O_2 we did not find significant differences among the groups but, in cells challenged with 3 mM H_2O_2 we observed both, for single and repeatedly treated cells, a significantly higher survival rate for cells treated with 6 μM ARI than the basal non-treated cells (Figure 1d,e), suggesting that ARI enhances survival also following a single treatment (Figure 1d). Finally, we further tested cell viability using a lactate dehydrogenase (LDH) release test, that measures cell rupture by determining the activity of LDH present in the extracellular media. Using this assay, we found that in single-treated cells, following a 3 mM H_2O_2 challenge, which increased LDH levels in non-treated cells, 6 μM ARI-treated cells had significantly lower LDH release than non-treated controls (Figure 1f) and in repeatedly-treated cells, where both 1.5 and 3 mM H_2O_2 increased LDH release in non-treated cells, following a 1.5 mM H_2O_2 challenge, 6 μM ARI-treated cells also had significantly lower LDH release than non-treated controls (Figure 1g). Altogether, these

data support that ARI enhances cell survival following an H_2O_2 challenge, while OLA if any, has the opposite effect. Of note, as previously reported, at baseline (without H_2O_2) 6 μM ARI, in both single and repeated treatments, significantly reduces MTT activity (Figure 1d,e). As there is no corresponding decrease in NR or increase in LDH release, this reduction is possibly related to ARI mitotoxicity.

Apoptosis. Since oxidative stress can lead to different types of cell death, including apoptosis, necroptosis, pyroptosis and ferroptosis [52], we decided to determine if the activation of apoptosis following the H_2O_2 challenge differed with the ARI/OLA pre-treatment. To that end, we evaluated the activity of Caspase 9, mainly involved in the mitochondrial cell death pathway, and the final effectors of apoptosis, Caspase 3/7. As previously reported, Fao cells both single- and repeatedly-treated with 2.23 μM ARI have significantly higher Caspase 9 activity at baseline (without H_2O_2) (Figure 2a,b). Even though Caspase 9 activity was lower in H_2O_2-treated cells than in baseline samples, we consistently found that both single and repeated treatment with 2.23 μM ARI also significantly maintained higher Caspase 9 activity compared to equally treated controls in 1.5 mM H_2O_2 challenged cells (Figure 2a,b). Furthermore, 6 μM ARI had the same effect in repeatedly treated cells, while these effects were not observed following treatment with OLA (Figure 2a,b). Nevertheless, when cells were challenged with 3 mM H_2O_2 both 6 μM ARI and 6 μM OLA in repeated treatment maintained higher Caspase 9 levels than those of untreated cells (Figure 2a,b). These results imply that the pro-survival activity of ARI is not related to a larger reduction in mitochondria-induced apoptosis. In fact, the observation that ARI-treated cells consistently show more Caspase 9 activity may relate to the higher levels of mitochondrial ROS and lower mitochondrial activity observed following ARI treatment.
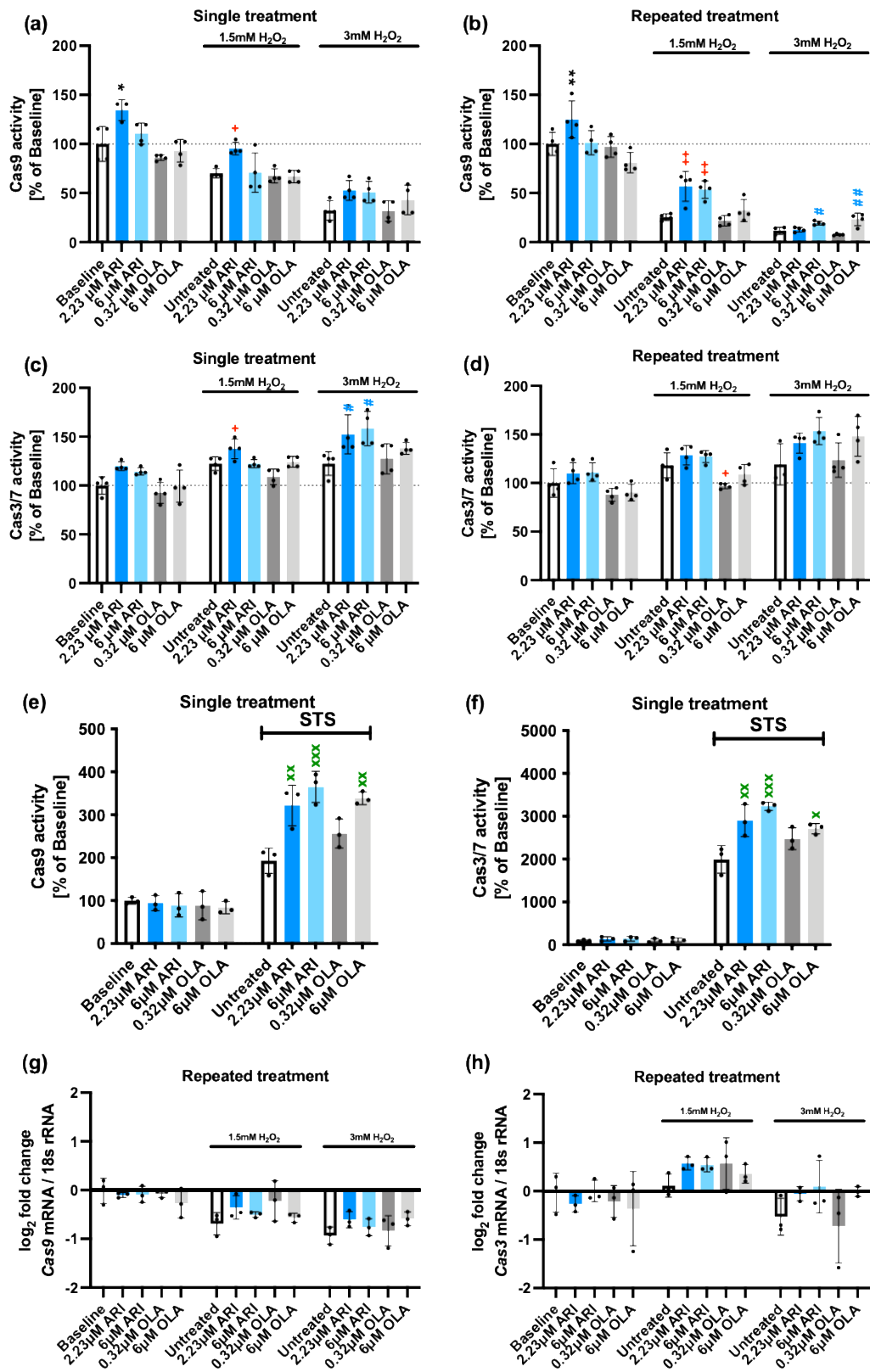
Figure 2. *Caspases levels and activities.* Caspase 9 activity in single- (**a**) and repeatedly- (**b**) treated Fao cells, challenged with H_2O_2. Caspase 3/7 activity in single- (**c**) and repeatedly- (**d**) treated Fao cells challenged with H_2O_2. Caspase 9 and 3/7 activities baseline data (without H_2O_2) in single- and repeatedly-treated cells (**a-d**) are re-used under CC-BY4.0 license [49]. Caspase 9 (**e**) and 3/7 activity (**f**) in single-treated Fao cells challenged with staurosporine (STS). Gene expression analysis of *Caspase 9* (g) and *Caspase 3* (h). Data are presented as mean ± SD and analyzed by one-way ANOVA followed by Dunnett's test, comparing samples within each group: non-treated to treated, without H_2O_2 (*),

non-treated to treated, challenged with 1.5 mM H_2O_2 (+); non-treated to treated, challenged with 3 mM H_2O_2 (#). Additionally, samples were analyzed with Tukey's test to compare 6 μM ARI to 6 μM OLA (**e**) and (**f**): Dunnett's test was used to test the comparison between the AAPs treatments with STS to untreated control with STS (x). ***/+/#/x**$p \leq 0.05$, ****/++/##/xx**$p \leq 0.01$, **xxx**$p \leq 0.001$. (a-d): $n = 4$; (e-h): $n = 3$. Cas: caspase.

We next evaluated Caspase 3/7 activities and, consistent with the results found for Caspase 9, we found that following a challenge with 1.5 or 3 mM H_2O_2, Fao cells, exposed to a single treatment with 2.23 μM ARI, maintained higher Caspase 3/7 levels than untreated controls (Figure 2c). Also, a single treatment with 6 μM ARI significantly showed higher Caspase 3/7 activity than untreated cells, in response to a 3 mM H_2O_2 challenge (Figure 2c). Similar tendencies were found in repeatedly-treated cells although in this case, differences did not reach statistical significance (Figure 2d). In contrast, following a challenge with 1.5 mM H_2O_2, cells repeatedly treated with 0.32 μM OLA had significantly lower Caspase 3/7 activity than untreated controls, which may suggest that OLA is somehow preventing apoptosis. In sum, these results suggest that ARI-treated cells are more sensitive to apoptotic cell death through the mitochondrial pathway while OLA at low doses can actually exert a protective effect even though at high doses it can also promote apoptotic cell death in H_2O_2-treated cells. These observations may relate to the higher levels of mitochondrial ROS in ARI-treated cells, and further suggest the concept that ARI pro-survival effects are not likely related to the regulation of apoptosis.

To determine if these apoptotic responses were specific for H_2O_2 exposure or similarly responsive to other pro-apoptotic stimuli, cells were exposed to staurosporine (STS) following a single treatment with ARI/OLA. All treatments were statistically significant compared to the baseline. Furthermore, we found that treatment with both 2.23 and 6 μM ARI, as well as 6 μM OLA increased Caspase 9 as well as Caspase 3/7 activities in response to STS administration (Figure 2e,f). This result confirms that both ARI and OLA have a general pro-apoptotic effect. Even though differences for the ARI *vs* OLA did not reach statistical significance, the observation that, on average, both Caspase 9 and Caspase 3 levels were higher for 6 μM ARI treated cells than for 6 μM OLA following STS administration are consistent with the previous data indicating that ARI is a stronger inducer of cell apoptosis than OLA.

We next determined if the cells were responding to the treatments and the H_2O_2 challenge modifying the two Caspases' gene expression. In repeatedly treated cells both at baseline and following 1.5/3 mM H_2O_2 exposure, we were unable to detect significant changes derived from the treatments. Nevertheless, 1.5/3 mM H_2O_2 exposure *per se* resulted in a small, significant, downregulation of *Caspase 9* expression (g) and 1.5 mM H_2O_2 induced a small, non-significant, upregulation of *Caspase 3* (h). Therefore, we concluded that ARI/OLA treatments do not affect Caspase's 9 and 3 gene expression.

In view of these observations, we decided to evaluate if the observed differences between ARI and OLA regarding their capacity to induce apoptotic cell death may be related to gene expression/protein level changes in other pro- or anti-apoptotic genes/proteins in repeatedly treated cells.

We first tested the anti-apoptotic BCL-2 family member BclXL [53] at gene expression (Figure 3a) and protein levels (Figure 3b). BclXL protein levels and mRNA levels were reduced in response to H_2O_2 in non-treated cells. In response to the treatments we found that, at baseline conditions 6 μM ARI significantly reduced its protein levels, although it did not alter its gene expression, suggesting this event was post-transcriptional. Following exposure to 1.5 mM H_2O_2 we found that cells treated with 2.23 μM ARI maintained higher mRNA and protein levels of BclXL than untreated controls, implying that these changes were transcriptionally regulated, with untreated cells being susceptible to a downregulation, while ARI-treated cells were more resistant to it. No significant differences were observed in response to OLA. Altogether these results suggest that if BclXL is a relevant factor in the higher capacity of ARI-treated cells to induce Caspase 9 activation, this would be likely related to the lower levels of BclXL in the ARI-treated cells at baseline, prior to H_2O_2 exposure. They also suggest that it is a lack of responsiveness in ARI treated cells that affects *Bclxl* transcriptional regulation.

Other anti-apoptotic BCL-2 family members were also evaluated at gene expression level: *Bcl2* and *Mcl1*. Regarding *Bcl2*, we found no differences in baseline levels among treatments nor following the challenge with 1.5/3 mM H_2O_2. Nevertheless, H_2O_2 induced a downregulation of the gene at the two doses tested, similar to what was observed for BclXL. Regarding *Mcl1*, we found no differences in baseline levels among treatments. Following the challenge with 1.5 mM H_2O_2 we found in non-treated cells a significant upregulation that was not modified by the treatments. In contrast, *3 mM* H_2O_2 exposure did not result in an upregulation of Mcl1 in non-treated cells over baseline levels (Figure 3d). Of note, following the challenge with 3 mM H_2O_2, 6 µM ARI-treated cells showed higher *Mcl1* expression than both non-treated controls and 6 µM OLA-treated cells, implying that ARI maintained the cellular responsiveness to Mcl1 induction in this case. Altogether, these results indicate that, following H_2O_2 exposure, ARI-treated cells maintain higher anti-apoptotic gene expression levels than non-treated or OLA-treated cells despite their higher caspase activity.

To understand the significance of these findings, since apoptosis is governed to a large extent through the balance between pro- and anti-apoptotic factors, we analyzed at gene expression level two pro-apoptotic members of the Bcl-2 family, *Bid* (Figure 3e) and *Bax* (Figure 3f) and another pro-apoptotic factor, *Diablo* [54] (Figure 3g). We found that *Bid* expression levels at baseline were similar among treatments, but following exposure to 1.5 mM H_2O_2 we observed that cells treated with 6 µM ARI maintained its higher expression levels. Non-treated cells when exposed to 3 mM H_2O_2 reduced B*id* levels and treated with either 2.23 or 6 µM ARI had higher *Bid* levels than non-treated controls, while OLA-treated cells did not significantly differ from non-treated controls. When *Bax* and *Diablo* gene expression were tested, we found that, 3 mM H_2O_2 decreased *Bax* levels and both 1.5 and 3 mM H_2O_2 decreased *Diablo* in non-treated cells. ARI-treated cells did not significantly alter the response tendency to reduce *Bax* and *Diablo* expression levels in the presence of H_2O_2, while 6 µM OLA-treated cells maintained significantly higher expression levels of both *Bax* and *Diablo* in the cells challenged with 3 mM H_2O_2. Furthermore, the higher OLA-dependent expression of *Diablo* was statistically significant compared to that of ARI (Figure 3g). Altogether, these results imply that following H_2O_2 exposure, ARI/OLA treated cells maintain higher expression levels of both pro- and anti-apoptotic genes, possibly making them more sensitive to both pro- and anti-apoptotic stimuli. The impact of ARI and OLA is different, and gene-specific. If the overall pro-/anti- apoptotic balance is globally altered by any of the antipsychotics remains to be established.
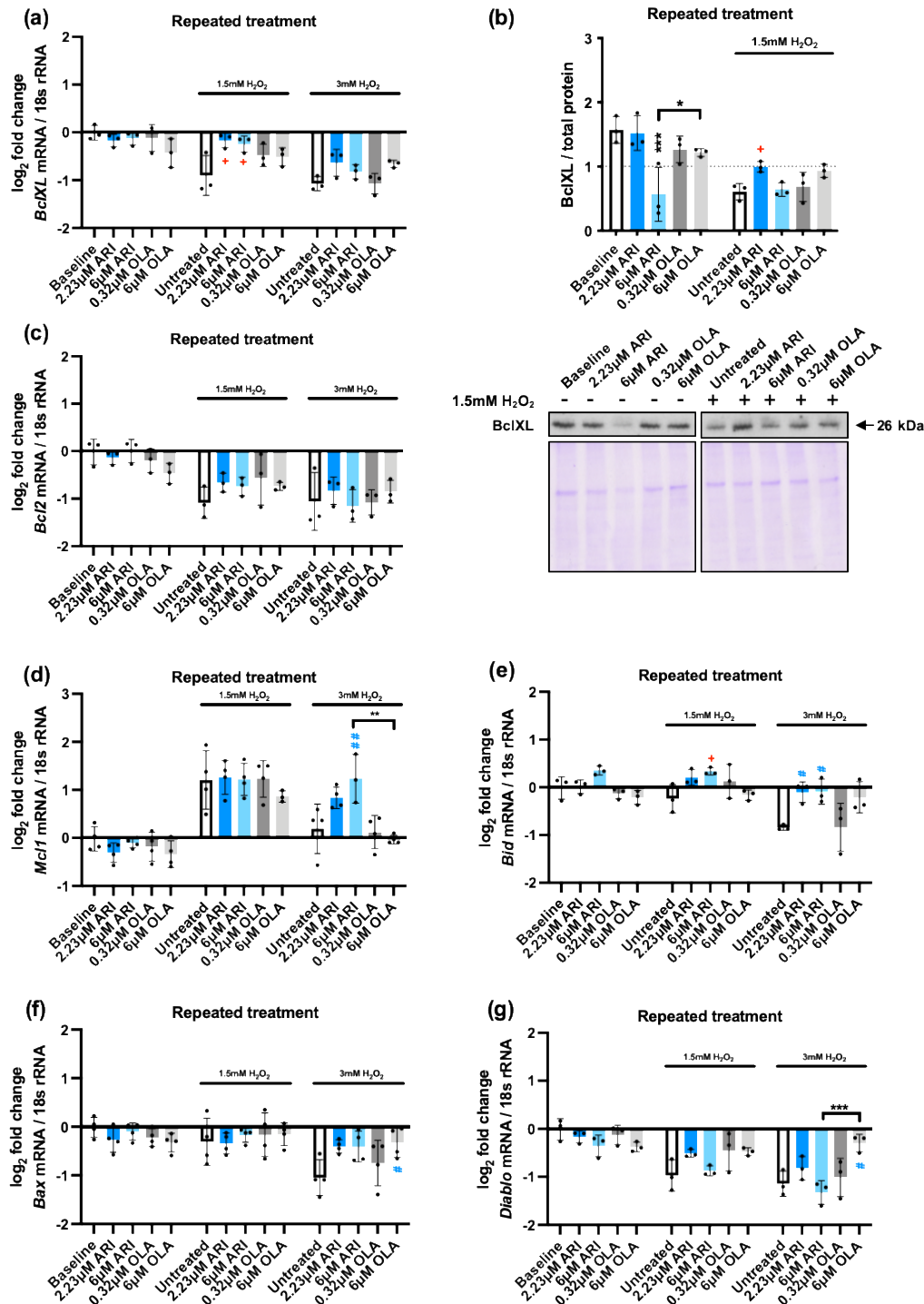
Figure 3. *Pro- and anti-apoptotic factors.* Log$_2$ fold-change in mRNA expression levels of pro- and anti-apoptotic factors in repeatedly treated Fao cells: (**a**) *BclXL*, (**c**) *Bcl2*, (**d**), *Mcl1* (**e**) *Bid,* (**f**) *Bax* and (**g**) *Diablo.* (**b**) BclXL western blot analysis and corresponding Coomassie blue stained gel (loading control). Data are presented as mean ± SD and analyzed by one-way ANOVA followed by Dunnett's test, comparing samples within each group: non-treated to treated, without H$_2$O$_2$ (*), non-treated to treated, challenged with 1.5 mM H$_2$O$_2$ (+); non-treated to treated, challenged with 3 mM H$_2$O$_2$ (#). Additionally, samples were analyzed with Tukey's test to compare 6 µM ARI to 6 µM OLA samples (* above the line indicating the comparison). */+/#$p \leq 0.05$, ##$p \leq 0.01$, ***$p \leq 0.001$. (**a, b, c, f, g**): $n = 3$; (**d, e**): $n = 4$.

The cellular response to oxidative stress also largely depends on the activation of mitogen activated protein kinases (MAPKs). In fact, their activity determines if the increased ROS levels can

drive increased cell proliferation, the activation of other stress response nodes, or cell death [55]. We, therefore, evaluated the activation of the three main stress kinases: p38, c-Jun amino-terminal kinases (JNKs), and extracellular signal regulated kinase (ERK1/2) (Figure 4) in response to 1.5 and 3 mM H_2O_2 exposure in cells repeatedly treated with ARI/OLA, testing their phosphorylation status by western blot. As expected, both 1.5 and 3 mM H_2O_2 exposure significantly increased phosphorylation of the three MAPKs. p38 is a multifaceted stress-responsive protein, well known as a ROS and DNA damage-sensitive protein that induces cell cycle arrest and regulates apoptosis [56]. p38 total protein levels were not modified at baseline by the treatments (Figure 4a-b) nor, in most cases, in response to H_2O_2 exposure, except for cells treated with 6 μM OLA exposed to 3 mM H_2O_2. Regarding p38 activation, cells treated with 6 μM OLA and 1.5/3 mM H_2O_2 also showed significantly higher p38 phosphorylation levels than non-treated cells (Figure 4c-d). Furthermore, in cells exposed to both 1.5 and 3 mM H_2O_2, that increased p38 phosphorylation in non-treated cells, there was a significant difference between 6 μM OLA and 6 μM ARI treated cells, with 6 μM OLA inducing higher p38 phosphorylation levels (Figure 4c-d). We next evaluated *p38* gene expression levels and found that, at baseline (without H_2O_2), the treatments did not modify p38 expression (Figure 4e). 1.5 and 3 mM H_2O_2 exposure induced a significant downregulation, which was partially prevented by ARI/OLA treatments. The response to 1.5 mM H_2O_2 was not significantly modified by the treatments, but in cells challenged with 3 mM H_2O_2 both, 2.23 μM ARI and 6 μM OLA maintained significantly higher levels of *p38* mRNA than non-treated controls (Figure 4e). Therefore, the observed hypersensitivity to p38 phosphorylation induced by OLA and its difference with ARI cannot be attributable to gene expression changes, since both treatments seem to promote the maintenance of *p38* levels. Notably, this gene expression pattern is remarkably similar to what was previously observed for pro- and anti-apoptotic factors except *Mcl1.*
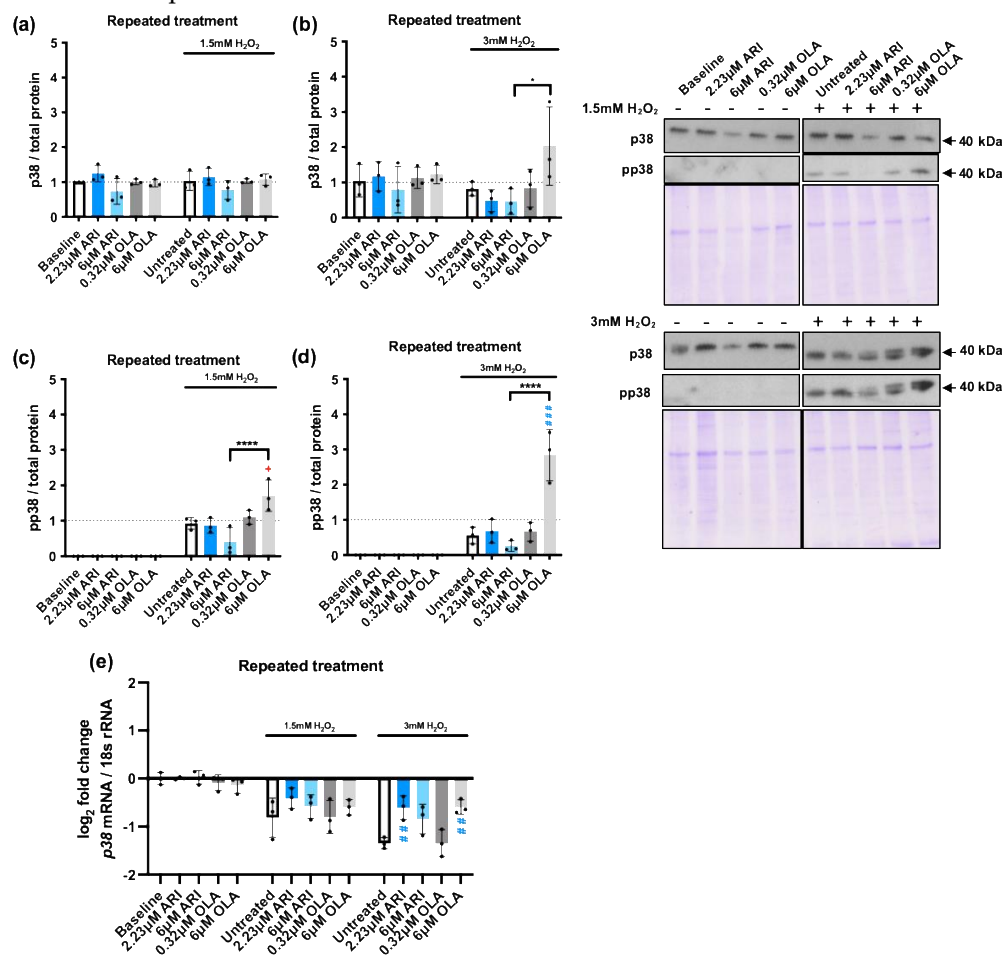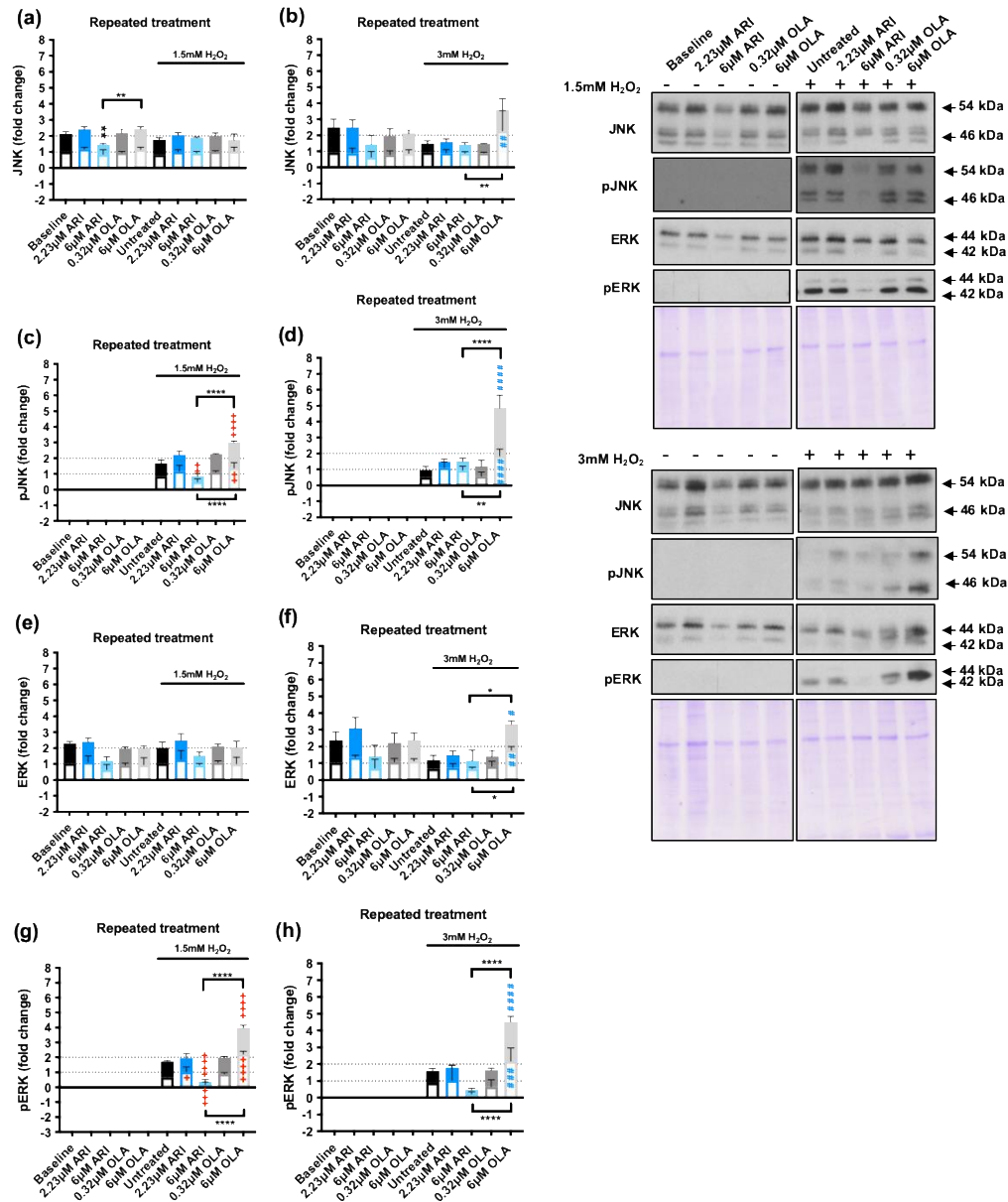

Figure 4. *MAPKs:* p38. (**a-b**) WB analysis of total p38 levels in cells challenged with 1.5 mM (**a**) or 3 mM (**b**) H_2O_2. (**c-d**) WB analysis of phospho-p38 (pp38) in cells challenged with 1.5 mM (**c**) or 3 mM (**d**) H_2O_2. Panels include graphs and representative western blots and corresponding Coomassie blue

dyed gels. (**e**) Logarithmic fold-change in mRNA expression levels of *p38*. Data are presented as mean ± SD and analyzed by one-way ANOVA followed by Dunnett's test, comparing samples within each group: non-treated to treated, without H_2O_2 (*), non-treated to treated, challenged with 1.5 mM H_2O_2 (+); non-treated to treated, challenged with 3 mM H_2O_2 (#). Additionally, samples are analyzed with Tukey's test, comparing 6 μM ARI to 6 μM OLA samples (*above the line indicating the comparison). */+$p \leq 0.05$, ##$p \leq 0.01$, ###$p \leq 0.001$, ****$p \leq 0.0001$; (**a-e**): $n = 3$.

We next evaluated JNK, a MAPK that can promote both cell survival and apoptosis in response to oxidative stress [57] as well as ERK1/2, a MAPK with well-known proliferative and protective effects on cells exposed to oxidative stress [58]. We tested JNK protein levels and activation in response to repeated treatments followed by H_2O_2 1.5/3 mM challenge (Figure 5) and observed that, at baseline conditions, 6 μM ARI significantly reduced JNK levels over those of non-treated cells, and this effect was not observed following 6 μM OLA treatment (Figure 5a-b). In contrast, JNK levels were increased following the 3 mM H_2O_2 challenge in 6 μM OLA treated cells, and in these conditions the difference between the 6 μM ARI and 6 μM OLA treated cells was significant. Consistently, JNK phosphorylation in response to 1.5 mM H_2O_2 was significantly reduced in cells treated with 6 μM ARI and enhanced in cells treated with 6 μM OLA, with differences among the two being statistically significant (Figure 5c). Furthermore, JNK phosphorylation in response to 3 mM H_2O_2 was increased in 6 μM OLA treated cells and the difference between 6 μM ARI and 6 μM OLA treated cells was also statistically significant (Figure 5d). Therefore, the effects of ARI and OLA on p38 and JNK were consistent with ARI reducing and OLA enhancing the response to H_2O_2.

Similarly, although in baseline conditions ERK1/2 levels were not significantly modified by any of the treatments (Figure 5e-f) in cells challenged with 3 mM H_2O_2, 6 μM OLA treated cells had significantly higher levels of ERK1/2 than non-treated controls as well as than 6 μM ARI treated cells. Also, the level of ERK1/2 phosphorylation in response to 1.5 mM H_2O_2 was significantly lower in 6 μM ARI than in non-treated controls, while the levels of ERK1/2 phosphorylation in response to 1.5/3 mM H_2O_2 where significantly higher in 6 μM OLA treated cells than in non-treated controls or than in cells treated with 6 μM ARI (Figure 5g-h). In sum, while treatment with 6 μM ARI reduced JNK and ERK levels activation in response to an oxidative stress challenge, 6 μM OLA treatment increased p38, JNK, and ERK1/2 activation in response to H_2O_2, indicating that while ARI tends to reduce MAPKs responsiveness to H_2O_2 exposure, OLA treatment has the opposite effect; this result is consistent with the changes observed in pro- and anti-apoptotic factors. These effects may be related to the basal oxidative stress levels that the cells are exposed to since ROS levels can alter the activity of regulatory phosphatases, peroxiredoxins, and tyrosine kinases, reducing the sensibility of signal transduction systems [59].
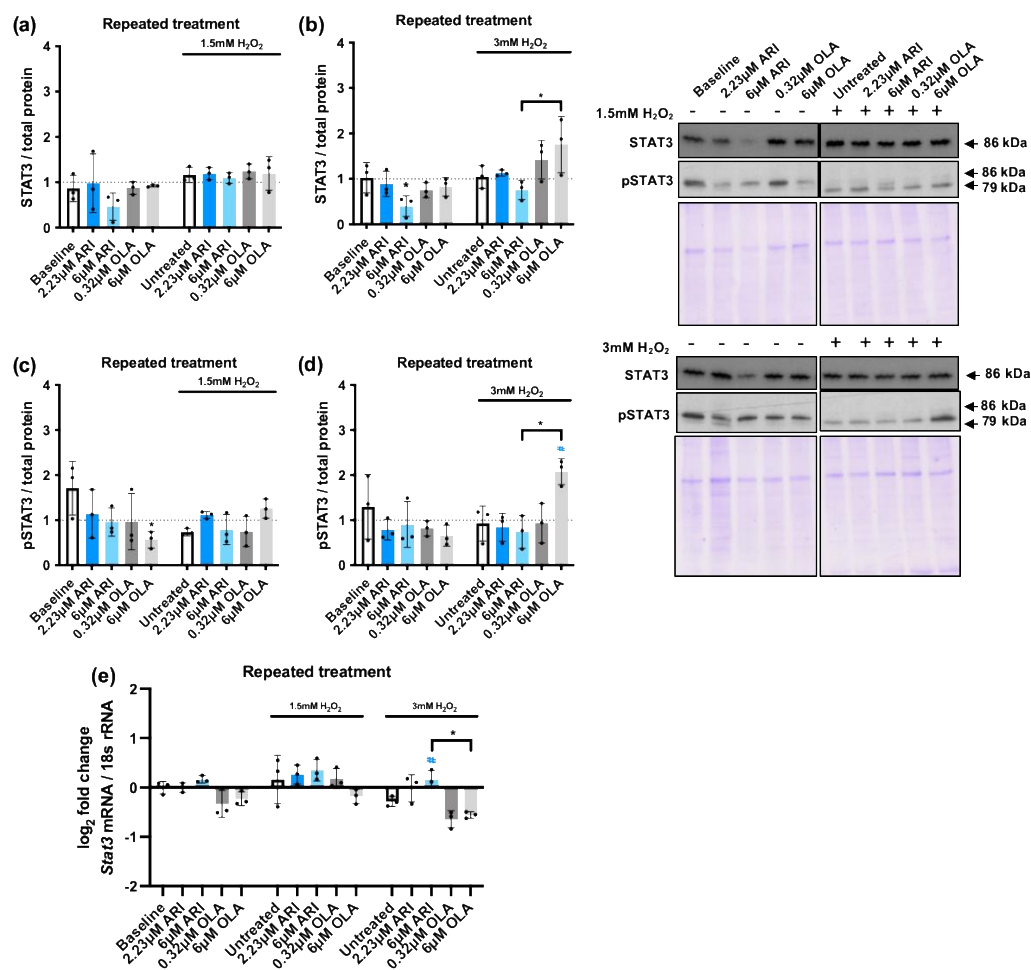
Figure 5. *MAPKs: JNK & ERK1/2.* (**a-b**) WB analysis of total JNK levels in cells challenged with 1.5 mM (**a**) or 3 mM (**b**) H_2O_2. (c-d) WB analysis of phospho-JNK (pJNK) in cells challenged with 1.5 mM (**c**) or 3 mM (**d**) H_2O_2. (**e-f**) WB analysis of total ERK1/2 levels in cells challenged with 1.5 mM (**e**) or 3 mM (**f**) H_2O_2. (**g-h**) WB analysis of phospho-ERK1/2 (pERK) in cells challenged with 1.5 mM (g) or 3 mM (h) H_2O_2. Panels include graphs and representative western blots and corresponding Coomassie blue dyed gels. Data are presented as mean ± SD and analyzed by one-way ANOVA followed by Dunnett's test, comparing samples within each group: non-treated to treated, without H_2O_2 (*), non-treated to treated, challenged with 1.5 mM H_2O_2 (+); non-treated to treated, challenged with 3 mM H_2O_2 (#). Additionally, samples are analyzed with Tukey's test, comparing 6 μM ARI to 6 μM OLA samples (*above the line indicating the comparison). */+/#$p \leq 0.05$, **/++/##$p \leq 0.01$, ***/###$p \leq 0.001$, ****/++++/####$p \leq 0.0001$; (a-h): $n = 3$. Legend: filled box reepresents JNK 46 (**a, b**), pJNK 46 (**c, d**), ERK 42, i.e. ERK2 (**e, f**) and pERK 42 (**g, h**). Empty box represents JNK 54 (**a, b**), pJNK 54 (**c, d**), ERK 44, i.e. ERK1 (**e, f**) and pERK 44 (**g, h**).

Another key mediator of the cellular response to stress is the transcription factor STAT3 [60], which generally plays a cytoprotective role preventing cellular apoptosis [61]. The cross-talk of MAPKs and STAT3 signaling pathways is crucial during the cellular response to oxidative stress [62]. Therefore, we analyzed STAT3 levels in repeatedly treated cells and we found a possibly relevant reduction at baseline in cells treated with 6 ®M ARI. In cells challenged with 3 mM H_2O_2 the levels of

STAT3 were found to be significantly higher in 6 μM OLA treated cells than in 6 μM ARI treated cells (Figure 6b). Next, we evaluated STAT3 activity analyzing its phosphorylation. Consistently, we found that STAT3 phosphorylation following the challenge with 3 mM H_2O_2 was higher in 6 μM OLA treated cells than in 6 μM ARI treated cells (Figure 6d). Finally, we analyzed *Stat3* gene expression that was reduced by H_2O_2 exposure in non-treated cells   and, although we did not find differences at baseline among the groups, 3 mM H_2O_2 exposure reduced *Stat3* levels more in cells treated with 6 μM OLA than in cells treated with 6 μM ARI. These results, along with the previously observed changes in MAPK activity and pro- and anti- apoptotic factor regulation, imply that overall ARI reduces while OLA enhances stress sensitivity, and change in responsiveness affects pro-survival and pro-apoptotic pathways. Notably, while ARI-dependent reduced sensitivity could be related to the observed oxidative stress, known to reduce the sensitivity of many signaling pathways, and in particular Tyr-receptor signaling, the mechanism involved in OLA-dependent enhanced sensitivity would need to be clarified.

Figure 6. *STAT3.* (**a-b**) WB analysis of total STAT3 levels in cells challenged with 1.5 mM (**a**) or 3 mM (**b**) H_2O_2. (**c-d**) WB analysis of phospho-STAT3 (pSTAT3) in cells challenged with 1.5 mM (**c**) or 3 mM (**d**) H_2O_2. Panels include graphs and representative western blots and corresponding Coomassie blue dyed gels. (**e**) Logarithmic fold-change in mRNA expression levels of *Stat3*. Data are presented as mean ± SD and analyzed by one-way ANOVA followed by Dunnett's test, comparing samples within each group: non-treated to treated, without H_2O_2 (*), non-treated to treated, challenged with 1.5 mM H_2O_2 (+); non-treated to treated, challenged with 3 mM H_2O_2 (#). Additionally, samples are analyzed with Tukey's test, comparing 6 μM ARI to 6 μM OLA samples (*above the line indicating the comparison). */#$p \leq 0.05$; (a-e): $n = 3$.

Since alteration of mitochondrial function seemed to be the primary driver in the differential response to H_2O_2, we next decided to determine if the mitochondrial load or the mitochondrial turnover were modified by repeated ARI or OLA treatments, since oxidative-stress damaged

mitochondria should be targeted to mitophagy, a specialized form of autophagy, and mitochondrial biogenesis should be activated to compensate for the loss [24] to maintain the cellular energy balance. Total mitochondrial content was determined by WB with antibodies directed against the mitochondrial protein Tim23, part of the TIM23 complex, localized in the inner mitochondrial membrane (IMM), that drives mitochondrial protein import into the IMM and the mitochondrial matrix [63]. We did not find any differences among the groups either at baseline or in response to 1.5/3 mM H_2O_2 (Figure 7a-b). Detection of mitophagy by this method was confirmed in conditions of starvation-induced mitophagy (Supplementary Figure 3a). We next evaluated autophagy by WB analysis of microtubule-associated protein 1A/1B-light chain 3 (LC3B). The cytosolic form of LC3B (LC3BI) is recruited to the phagosome membranes following conjugation with phosphatidylethanolamine, forming LC3BII. Therefore, the LC3BI/II ratio is commonly used as an indicator of autophagy flux. We found that cells treated with 6 μM OLA both at baseline and following a challenge with 3 mM H_2O_2, maintained significantly higher levels of LC3BI than corresponding non-treated controls, while ARI significantly modified LC3BI levels in all of the conditions tested (Figure 7c-d). In cells challenged with 1.5 mM H_2O_2, 6 μM ARI treatment significantly increased the levels of LC3BII, while 6 μM OLA treated cells had significantly lower LC3BII levels than non-treated controls (Figure 7e-f). These results suggest that ARI treated cells may have an enhanced autophagy flux, likely to remove damaged mitochondria exposed to high levels of $O_2^{\bullet-}$ while OLA treatment leads to a reduction in the levels of autophagy.
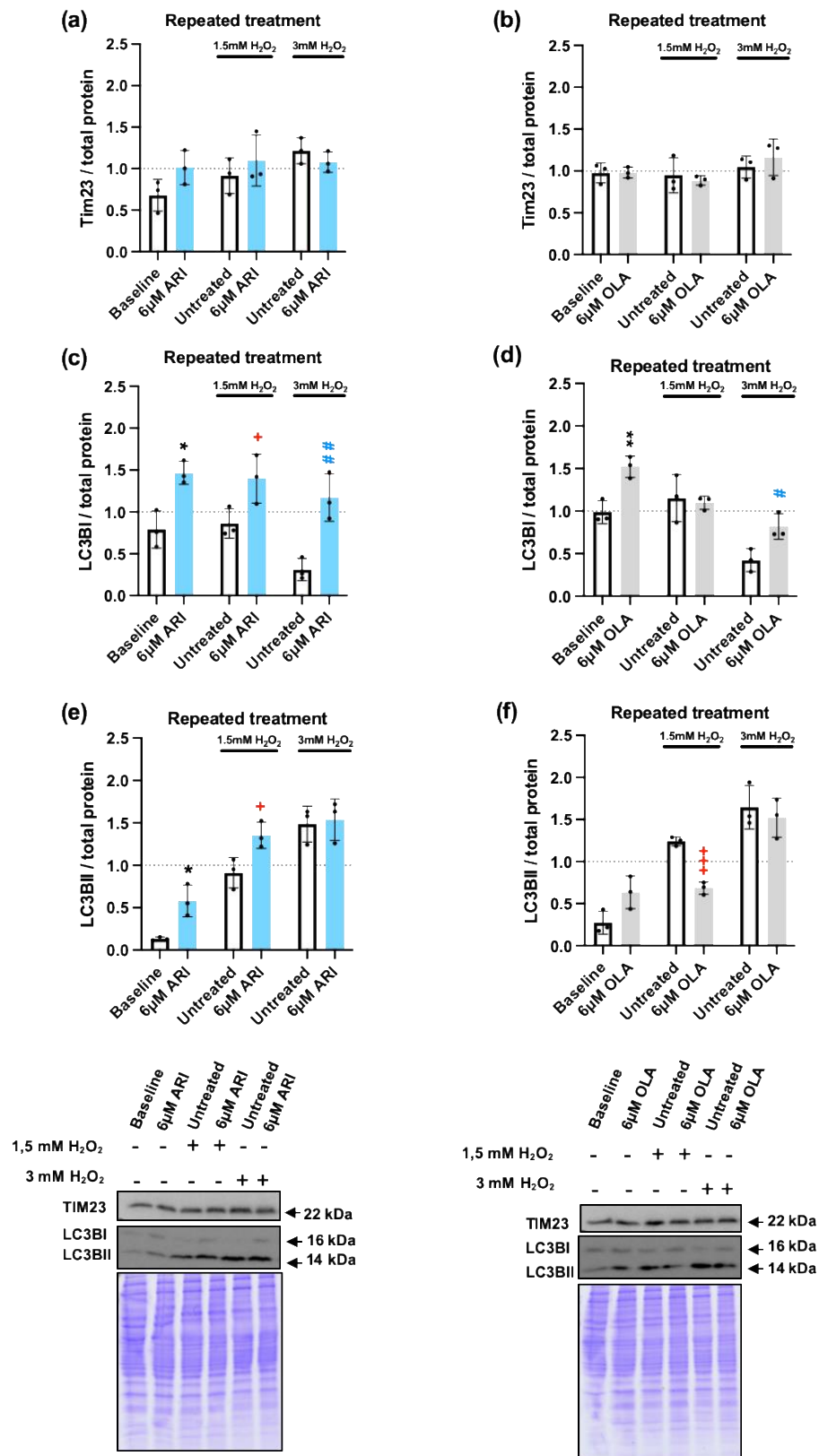
Figure 7. *Mitochondria load and Autophagy.* (a-b) WB analysis of Tim23 in cells treated with ARI (**a**) or OLA (**b**) and then challenged with 1.5/3 mM H_2O_2. (c-d) WB analysis of LC3BI in cells treated with ARI (**c**) or OLA (**d**) and then challenged with 1.5/3 mM H_2O_2. (**e-f**) WB analysis of LC3BII in cells treated with ARI (**e**) or OLA (**f**) and then challenged with 1.5/3 mM H_2O_2. Panels include graphs and representative western blots and corresponding Coomassie blue dyed gels. Data are presented as mean ± SD and analyzed with Unpaired *t* test, comparing samples within each group: non-treated to

treated, without H_2O_2 (*), non-treated to treated, challenged with 1.5 mM H_2O_2 (+); non-treated to treated, challenged with 3 mM H_2O_2 (#).*/+/#$p \leq 0.05$, **/+/##$p \leq 0.01$, +++$p \leq 0.001$; (a-f): $n = 3$.

Elevated ROS levels increase the cellular load of oxidized/damaged proteins that should be targeted for degradation by the proteasome, however, both ROS themselves and the reduction of mitochondrial oxidative capacity can negatively impact the proteasome activity, leading to the accumulation of damaged proteins and eventually drive the limitation of cellular functionality and even cell death [64][65]. There are two main proteasome complexes, the 26S complex activity, which requires ATP and targets ubiquitinated proteins, and is responsible for ≥80% of the total proteasome activity [66]. The remaining 20% is degraded by the 20S proteasome complex that is both ubiquitin and ATP-independent [67]. Both 26S and 20S proteasome complexes can degrade oxidatively damaged proteins but the 20S complex is the main protease responsible for degrading oxidized proteins, likely because it is more resistant to ROS than the 26S complex [68]. Therefore, we decided to evaluate how ARI and OLA repeated treatment modified the proteasomal response to cells exposed to 1.5/3 mM H_2O_2. Basal proteasomal activity, following ATP addition (ATP+) and ATP depletion (ATP-) were determined as well as the ATP+/ATP- activity ratio. As previously reported [69], 3 mM H_2O_2 reduced both 26S (ATP-dependent) and 20S (ATP-independent) proteasome activity (Figure 8). Of note, neither depletion nor addition of ATP did significantly modify the inhibition rate, although 3 mM H_2O_2 produced a non-significant higher inhibition of the ATP dependent activity, with a lower ATP+/ATP- activity ratio (Figure 8d). ARI treatment did not significantly alter the ATP-dependent (26S) (Figure 8b) nor ATP-independent (20S) (Figure 8c) proteasome activities compared to baseline. However, 2.23 μM ARI significantly increased the ATP+/ATP- activity ratio (Figure 8d), suggesting a better maintenance of the 26S activity than of the 20S complex in this case. Importantly, 6 μM OLA treatment at 3mM H_2O_2 significantly increased proteasomal activity over that of the untreated cells, recovering the proteasomal activity levels observed in the absence of H_2O_2 (Figure 8b, c). These observations, suggest that OLA treatment has an important general protective role on the ROS-dependent inactivation of the proteasome by H_2O_2, while ARI treatment can have a small but significant effect on the maintenance of the 26S, that could be related to the higher levels of antioxidants over baseline. The protection elicited by OLA is likely more related to the lower load of damaged mitochondria [70] than to the higher sensitivity to MAPK activation, since p38 has been shown to inhibit proteasome activity [71].
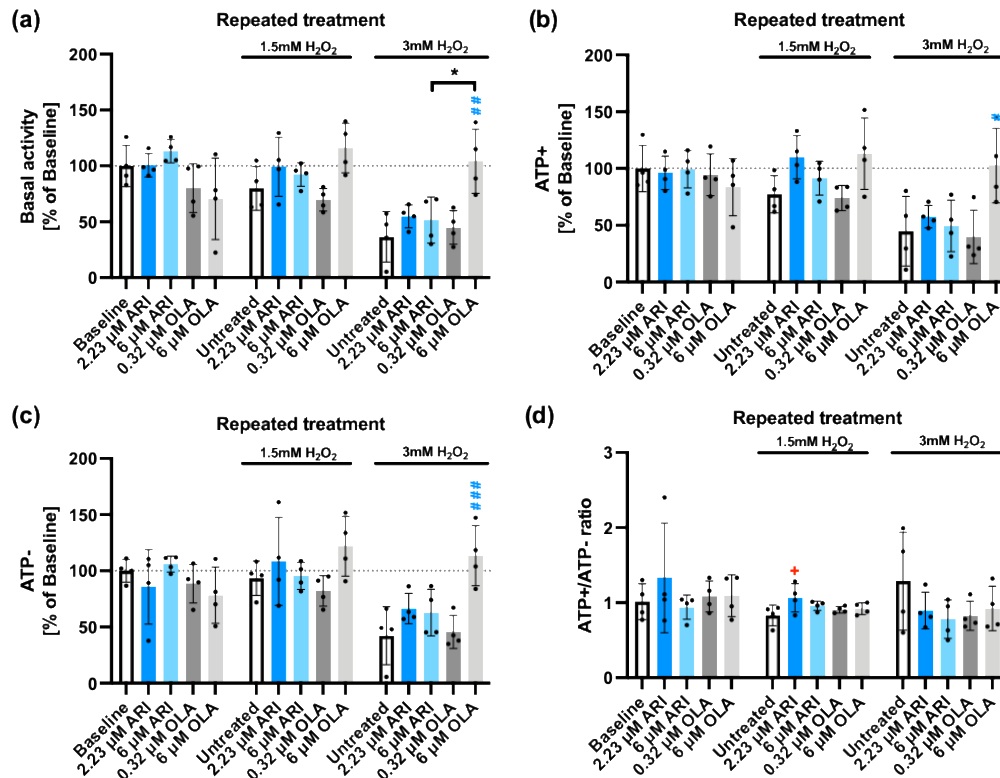
Figure 8. *Proteasome activity.* (a) basal conditions; (b) with added ATP, ATP+; (c) following ATP depletion, ATP-; (d) ratio of ATP+ vs ATP- activity determinations. Data are presented as mean ± SD and analyzed with one-way ANOVA followed by Dunnett's test, comparing samples within each group: non-treated to treated, without H_2O_2 (*), non-treated to treated, challenged with 1.5 mM H_2O_2 (+); non-treated to treated, challenged with 3 mM H_2O_2 (#). Additionally, samples are analyzed with Tukey's test, comparing 6 μM ARI to 6 μM OLA samples (*above the line indicating the comparison).*/+/#$p \leq 0.05$, ##$p \leq 0.01$, ###$p \leq 0.001$; (a-d): $n = 4$.

In summary, ARI treated cells produce higher levels of mitochondrial ROS, and induce more strongly mitophagy and mitochondria dependent apoptosis in responses to H_2O_2 exposure. However, these cells die less than controls, possibly because the stress signaling pathways are blunted, as suggested by the reduced activation of the MAPKs and STAT3 in stress conditions, as well as blunted gene expression changes in pro- and anti-apoptotic factors in response to ROS. In contrast, OLA treatment, reduces the mitophagy flux, hyper-sensitizes cells to stress signaling, and protects proteasomal activity in cells exposed to high ROS levels, suggesting it has a sensitizing effect driving effectively cell death in stress conditions despite of the reduced cellular damage.

4. Discussion

The potential hazards derived from the mitochondrial toxicity of pharmacological drugs are a rising concern, especially when the patient is under a lifelong treatment regime [72]. The nature of neuropharmacology is specially demanding in terms of penetrability, since neuropharmacological drugs have to cross the hemato-encephalic barrier (HEB). Also, circulating drug concentrations need to be relatively high to ensure they cross the HEB at therapeutic levels [73]. All these likely contribute to the observed increased incidence of metabolic diseases that can be attributable to the pharmacological treatments in patients [74]. Under terms such as *mitochondrial toxicity* or *mitochondrial dysfunction* lies a highly complex variety of possible biological effects derived from the incorporation of pharmacological drugs and the disruption of normal mitochondrial physiology. The variety of mitochondrial related pathological outcomes is well illustrated by the often puzzling phenotypical variety of mitochondrial genetic diseases [75]. Most importantly, up to date there are

no implemented protocols that can accurately evaluate these nor provide an effective risk assessment for disease development [76].

In this study we aimed to understand how two widely used AAPs, ARI and OLA that have been shown to inhibit mitochondria oxidative phosphorylation, alter cellular physiology in terms of changing their capacity to respond to stress. This notion is based on previous studies demonstrating that mitochondrial oxidative function is closely related to the control of the cellular capacity to respond to various types of stressors and thus provide an effective mechanism against disease in general [26,77].

Our study shows that ARI but not OLA treatment results in a higher level of mitochondrial oxidative stress, which is likely the driver of an enhanced mitophagy flux in ARI treated cells and is associated with a consistently higher sensitivity to mitochondria-driven apoptosis activation than non-treated controls. Oxidative stress has been shown to induce apoptosis in a wide variety, if not all, of cell types. However, ARI treated cells are actually less sensitive to changes normally induced in stress conditions. This lack of sensitivity includes the loss of transcriptional regulation of genes related to apoptosis control and a reduced activation of both MAPKs and STAT3, while OLA has the opposite effect. These observations are consistent with the known effect of persistent cellular oxidative stress, that can oxidatively inactivate key signaling mediators, including membrane receptors and regulatory phosphatases. Therefore, this lack of responsiveness in ARI treated cells is likely behind the observed reduced cell death rates.

In stark contrast, OLA treatment induces hypersensitivity to stress responses at all tested levels (gene expression of apoptosis regulators, MAPK and STAT3 activation, proteasome activity) that cannot be attributable to detectable differences in mitochondrial oxidative stress, as detected by MitoSOX labeling of $O_2^{\bullet-}$, to global changes in oxidative stress that would affect the 26S/20S activity ratio, nor to changes in mitochondrial levels, evaluated through the determination of Tim23 protein levels. Of note, OLA seemed to reduce autophagy in H_2O_2 treated cells or maybe more accurately, the induction of autophagy by H_2O_2 is reduced in OLA treated cells. This result may seem surprising since, in this conditions, OLA does not seem to have a higher antioxidant capacity than control cells [39], but it could be attributable to the increased activity of the proteasome detectable in challenged OLA treated cells, predictably increasing the cellular capacity to remove oxidatively damaged proteins.

The observed high proteasome activity can also be relevant for the observed hypersensitivity to MAPK activation in OLA treated cells. The connection between MAPK activation and proteasome activity is particularly well characterized in the case of ERK. ERK activation in response to oxidative stress has been shown to be dependent on the activity of the proteasome [78]. Proteosome inactivation blocks the activation of the ERK upstream kinase MEK [79].

Oxidative stress is a well-defined activator of the proteasome, however, chronic exposure to ROS and mitochondrial dysfunction tend to reduce the proteasome activity. The critical role of proteasome in ROS dependent effects is highlighted by its role in the activation of the inflammasome, a process that is also dependent on MAPK activation [80].

The observed higher proteasome activity in OLA treated cells exposed to H_2O_2 was not associated with any detectable differences in proteasome baseline levels nor in any significant changes in baseline MAPK levels or activity. Therefore, the origin of this conditioning effect remains to be established. Nevertheless, there is one detectable baseline difference in OLA treated cells, a significant increase in LC3BI levels that was not associated with a reduction in LCBII, and therefore, does not seem to be related to an inhibition of the autophagy flux, but may be rather indicative of an increased capacity of the cells to induce it and by extension to the degradation of damaged proteins/structures. Although highly speculative this may hold a connection with the high sensitivity of the proteasome activation in response to OLA. Furthermore, given the differential effects of ARI and OLA, it is tempting to speculate that mitochondrial function may play a role.

Total LC3 levels are regulated by acetylation, which prevents its degradation by the proteasome [81]. High LC3 levels have been shown in tumor tissues and are associated with advanced tumor stages and poor prognosis [82]. In fasting conditions, increased $NAD^+/NADH$ ratios activate the

deacetylase SIRT1 [83], rendering the protein more sensitive to proteasomal degradation but also activating the mitophagy flux since it facilitates its phosphatidylethanolamine (PE) conjugation to pre-autophagic membranes [84]. Therefore, high LC3B levels can be indicative of a good cellular nutritional and redox status. All these possibilities would need to be further investigated.

In sum, our observations highlight the divergent impacts that drug-induced mitochondrial toxicity can have on the physiological responses to stress, evidence the critical role played by chronic mitochondrial oxidative stress exposure in the cellular de-sensitization to stressors and raise a note of caution on the potential pathological outcomes of long-term ARI treatment.

References

1. Orsel, K.; Taipale, H.; Tolppanen, A.-M.; Koponen, M.; Tanskanen, A.; Tiihonen, J.; Gardarsdottir, H.; Hartikainen, S. Psychotropic Drugs Use and Psychotropic Polypharmacy among Persons with Alzheimer's Disease. *European Neuropsychopharmacology* **2018**, *28*, 1260–1269, doi:10.1016/j.euroneuro.2018.04.005.

2. Park, S.Y.; Cervesi, C.; Galling, B.; Molteni, S.; Walyzada, F.; Ameis, S.H.; Gerhard, T.; Olfson, M.; Correll, C.U. Antipsychotic Use Trends in Youth With Autism Spectrum Disorder and/or Intellectual Disability: A Meta-Analysis. *Journal of the American Academy of Child & Adolescent Psychiatry* **2016**, *55*, 456-468.e4, doi:10.1016/j.jaac.2016.03.012.

3. Birnbaum, M.L.; Saito, E.; Gerhard, T.; Winterstein, A.; Olfson, M.; Kane, J.M.; Correll, C.U. Pharmacoepidemiology of Antipsychotic Use in Youth with ADHD: Trends and Clinical Implications. *Curr Psychiatry Rep* **2013**, *15*, 382, doi:10.1007/s11920-013-0382-3.

4. Dennis, J.A.; Gittner, L.S.; Payne, J.D.; Nugent, K. Characteristics of U.S. Adults Taking Prescription Antipsychotic Medications, National Health and Nutrition Examination Survey 2013–2018. *BMC Psychiatry* **2020**, *20*, 483, doi:10.1186/s12888-020-02895-4.

5. Kaguelidou, F.; Holstiege, J.; Schink, T.; Bezemer, I.; Poluzzi, E.; Mazzaglia, G.; Pedersen, L.; Sturkenboom, M.; Trifirò, G. 'Use of Antipsychotics in Children and Adolescents: A Picture from the ARITMO Population-Based European Cohort Study.' *Epidemiology and Psychiatric Sciences* **2020**, *29*, e117, doi:10.1017/S2045796020000293.

6. Callaghan, J.T.; Bergstrom, R.F.; Ptak, L.R.; Beasley, C.M. Olanzapine. *Clin Pharmacokinet* **1999**, *37*, 177–193, doi:10.2165/00003088-199937030-00001.

7. Mauri, M.C.; Paletta, S.; Di Pace, C.; Reggiori, A.; Cirnigliaro, G.; Valli, I.; Altamura, A.C. Clinical Pharmacokinetics of Atypical Antipsychotics: An Update. *Clin Pharmacokinet* **2018**, *57*, 1493–1528, doi:10.1007/s40262-018-0664-3.

8. Carli, M.; Kolachalam, S.; Longoni, B.; Pintaudi, A.; Baldini, M.; Aringhieri, S.; Fasciani, I.; Annibale, P.; Maggio, R.; Scarselli, M. Atypical Antipsychotics and Metabolic Syndrome: From Molecular Mechanisms to Clinical Differences. *Pharmaceuticals* **2021**, *14*, 238, doi:10.3390/ph14030238.

9. Chow, R.T.S.; Whiting, D.; Favril, L.; Ostinelli, E.; Cipriani, A.; Fazel, S. An Umbrella Review of Adverse Effects Associated with Antipsychotic Medications: The Need for Complementary Study Designs. *Neuroscience & Biobehavioral Reviews* **2023**, *155*, 105454, doi:10.1016/j.neubiorev.2023.105454.

24

10. Rojo, L.E.; Gaspar, P.A.; Silva, H.; Risco, L.; Arena, P.; Cubillos-Robles, K.; Jara, B. Metabolic Syndrome and Obesity among Users of Second Generation Antipsychotics: A Global Challenge for Modern Psychopharmacology. *Pharmacological Research* **2015**, *101*, 74–85, doi:10.1016/j.phrs.2015.07.022.

11. Grajales, D.; Ferreira, V.; Valverde, Á.M. Second-Generation Antipsychotics and Dysregulation of Glucose Metabolism: Beyond Weight Gain. *Cells* **2019**, *8*, 1336, doi:10.3390/cells8111336.

12. Bernardo, M.; Rico-Villademoros, F.; García-Rizo, C.; Rojo, R.; Gómez-Huelgas, R. Real-World Data on the Adverse Metabolic Effects of Second-Generation Antipsychotics and Their Potential Determinants in Adult Patients: A Systematic Review of Population-Based Studies. *Adv Ther* **2021**, *38*, 2491–2512, doi:10.1007/s12325-021-01689-8.

13. Rotella, F.; Cassioli, E.; Calderani, E.; Lazzeretti, L.; Ragghianti, B.; Ricca, V.; Mannucci, E. Long-Term Metabolic and Cardiovascular Effects of Antipsychotic Drugs. A Meta-Analysis of Randomized Controlled Trials. *European Neuropsychopharmacology* **2020**, *32*, 56–65, doi:10.1016/j.euroneuro.2019.12.118.

14. Molina, J.D.; Avila, S.; Rubio, G.; López-Muñoz, F. Metabolomic Connections between Schizophrenia, Antipsychotic Drugs and Metabolic Syndrome: A Variety of Players. *Current Pharmaceutical Design* **2021**, *27*, 4049–4061, doi:10.2174/1381612827666210804110139.

15. Li, X.-Q.; Tang, X.-R.; Li, L.-L. Antipsychotics Cardiotoxicity: What's Known and What's Next. *World J Psychiatry* **2021**, *11*, 736–753, doi:10.5498/wjp.v11.i10.736.

16. Cuerda, C.; Velasco, C.; Merchán-Naranjo, J.; García-Peris, P.; Arango, C. The Effects of Second-Generation Antipsychotics on Food Intake, Resting Energy Expenditure and Physical Activity. *Eur J Clin Nutr* **2014**, *68*, 146–152, doi:10.1038/ejcn.2013.253.

17. Papatriantafyllou, E.; Efthymiou, D.; Markopoulou, M.; Sakellariou, E.-M.; Vassilopoulou, E. The Effects of Use of Long-Term Second-Generation Antipsychotics on Liver and Kidney Function: A Prospective Study. *Diseases* **2022**, *10*, 48, doi:10.3390/diseases10030048.

18. Baeza, I.; de la Serna, E.; Calvo-Escalona, R.; Merchán-Naranjo, J.; Rodríguez-Latorre, P.; Martínez-Cantarero, M.C.; Andrés, P.; Alda, J.A.; Muñoz-Samons, D.; Ilzarbe, D.; et al. One-Year Prospective Study of Liver Function Tests in Children and Adolescents on Second-Generation Antipsychotics: Is There a Link with Metabolic Syndrome? *Journal of Child and Adolescent Psychopharmacology* **2018**, *28*, 463–473, doi:10.1089/cap.2017.0117.

19. Todorović Vukotić, N.; Đorđević, J.; Pejić, S.; Đorđević, N.; Pajović, S.B. Antidepressants- and Antipsychotics-Induced Hepatotoxicity. *Arch Toxicol* **2021**, *95*, 767–789, doi:10.1007/s00204-020-02963-4.

20. Mortimer, K.R.H.; Katshu, M.Z.U.H.; Chakrabarti, L. Second-Generation Antipsychotics and Metabolic Syndrome: A Role for Mitochondria. *Front Psychiatry* **2023**, *14*, 1257460, doi:10.3389/fpsyt.2023.1257460.

21. Rosell-Hidalgo, A.; Eakins, J.; Walker, P.; Moore, A.L.; Ghafourian, T. Risk Assessment of Psychotropic Drugs on Mitochondrial Function Using In Vitro Assays. *Biomedicines* **2023**, *11*, 3272, doi:10.3390/biomedicines11123272.

22. Daniels, T.; Olsen, E.; Tyrka, A.R. Stress and Psychiatric Disorders: The Role of Mitochondria. *Annu Rev Clin Psychol* **2020**, *16*, 165–186, doi:10.1146/annurev-clinpsy-082719-104030.

23. Trigo, D.; Nadais, A.; Carvalho, A.; Morgado, B.; Santos, F.; Nóbrega-Pereira, S.; da Cruz E Silva, O.A.B. Mitochondria Dysfunction and Impaired Response to Oxidative Stress Promotes Proteostasis Disruption in Aged Human Cells. *Mitochondrion* **2023**, *69*, 1–9, doi:10.1016/j.mito.2022.10.002.

24. Doblado, L.; Lueck, C.; Rey, C.; Samhan-Arias, A.K.; Prieto, I.; Stacchiotti, A.; Monsalve, M. Mitophagy in Human Diseases. *Int J Mol Sci* **2021**, *22*, 3903, doi:10.3390/ijms22083903.

25. Romani, P.; Nirchio, N.; Arboit, M.; Barbieri, V.; Tosi, A.; Michielin, F.; Shibuya, S.; Benoist, T.; Wu, D.; Hindmarch, C.C.T.; et al. Mitochondrial Fission Links ECM Mechanotransduction to Metabolic Redox Homeostasis and Metastatic Chemotherapy Resistance. *Nat Cell Biol* **2022**, *24*, 168–180, doi:10.1038/s41556-022-00843-w.

26. Valle, I.; Álvarez-Barrientos, A.; Arza, E.; Lamas, S.; Monsalve, M. PGC-1α Regulates the Mitochondrial Antioxidant Defense System in Vascular Endothelial Cells. *Cardiovasc Res* **2005**, *66*, 562–573, doi:10.1016/j.cardiores.2005.01.026.

27. García-Quintans, N.; Sánchez-Ramos, C.; Prieto, I.; Tierrez, A.; Arza, E.; Alfranca, A.; Redondo, J.M.; Monsalve, M. Oxidative Stress Induces Loss of Pericyte Coverage and Vascular Instability in PGC-1α-Deficient Mice. *Angiogenesis* **2016**, *19*, 217–228, doi:10.1007/s10456-016-9502-0.

28. Li, H.; Peng, S.; Li, S.; Liu, S.; Lv, Y.; Yang, N.; Yu, L.; Deng, Y.-H.; Zhang, Z.; Fang, M.; et al. Chronic Olanzapine Administration Causes Metabolic Syndrome through Inflammatory Cytokines in Rodent Models of Insulin Resistance. *Sci Rep* **2019**, *9*, 1582, doi:10.1038/s41598-018-36930-y.

29. Huhn, M.; Nikolakopoulou, A.; Schneider-Thoma, J.; Krause, M.; Samara, M.; Peter, N.; Arndt, T.; Bäckers, L.; Rothe, P.; Cipriani, A.; et al. Comparative Efficacy and Tolerability of 32 Oral Antipsychotics for the Acute Treatment of Adults with Multi-Episode Schizophrenia: A Systematic Review and Network Meta-Analysis. *The Lancet* **2019**, *394*, 939–951, doi:10.1016/S0140-6736(19)31135-3.

30. Citrome, L.; McEvoy, J.P.; Todtenkopf, M.S.; McDonnell, D.; Weiden, P.J. A Commentary on the Efficacy of Olanzapine for the Treatment of Schizophrenia: The Past, Present, and Future. *NDT* **2019**, *Volume 15*, 2559–2569, doi:10.2147/NDT.S209284.

31. Alabaku, O.; Yang, A.; Tharmarajah, S.; Suda, K.; Vigod, S.; Tadrous, M. Global Trends in Antidepressant, Atypical Antipsychotic, and Benzodiazepine Use: A Cross-Sectional Analysis of 64 Countries. *PLoS ONE* **2023**, *18*, e0284389, doi:10.1371/journal.pone.0284389.

32. Bever, K.A.; Perry, P.J. Olanzapine: A Serotonin-Dopamine-Receptor Antagonist for Antipsychotic Therapy. *American Journal of Health-System Pharmacy* **1998**, *55*, 1003–1016, doi:10.1093/ajhp/55.10.1003.

33. Komossa, K.; Rummel-Kluge, C.; Hunger, H.; Schmid, F.; Schwarz, S.; Duggan, L.; Kissling, W.; Leucht, S. Olanzapine versus Other Atypical Antipsychotics for Schizophrenia. *Cochrane Database of Systematic Reviews* **2010**, doi:10.1002/14651858.CD006654.pub2.

34. Söderberg, M.M.; Dahl, M.-L. Pharmacogenetics of Olanzapine Metabolism. *Pharmacogenomics* **2013**, *14*, 1319–1336, doi:10.2217/pgs.13.120.

35. Zhu, Z.; Cao, T.; Chen, H.; Zhang, B.; Lin, C.; Cai, H. Olanzapine-Induced Nonalcoholic Fatty Liver Disease: The Effects of Differential Food Pattern and the Involvement of PGRMC1 Signaling. *Food and Chemical Toxicology* **2023**, *176*, 113757, doi:10.1016/j.fct.2023.113757.

36. del Campo, A.; Bustos, C.; Mascayano, C.; Acuña-Castillo, C.; Troncoso, R.; Rojo, L.E. Metabolic Syndrome and Antipsychotics: The Role of Mitochondrial Fission/Fusion Imbalance. *Frontiers in Endocrinology* **2018**, *9*.

37. Scaini, G.; Quevedo, J.; Velligan, D.; Roberts, D.L.; Raventos, H.; Walss-Bass, C. Second Generation Antipsychotic-Induced Mitochondrial Alterations: Implications for Increased Risk of Metabolic Syndrome in Patients with Schizophrenia. *European Neuropsychopharmacology* **2018**, *28*, 369–380, doi:10.1016/j.euroneuro.2018.01.004.

38. Eftekhari, A.; Azarmi, Y.; Parvizpur, A.; Eghbal, M.A. Involvement of Oxidative Stress and Mitochondrial/Lysosomal Cross-Talk in Olanzapine Cytotoxicity in Freshly Isolated Rat Hepatocytes. *Xenobiotica* **2016**, *46*, 369–378, doi:10.3109/00498254.2015.1078522.

39. Pirc Marolt, T.; Kramar, B.; Vovk, A.; Podgornik, H.; Šuput, D.; Milisav, I. Therapeutic Dosage of Antipsychotic Drug Aripiprazole Induces Persistent Mitochondrial Hyperpolarisation, Moderate Oxidative Stress in Liver Cells, and Haemolysis : Research Data Underlying the Article Available online: https://repozitorij.uni-lj.si/IzpisGradiva.php?id=151979 (accessed on 21 February 2024).

40. Cikánková, T.; Fišar, Z.; Bakhouche, Y.; Ľupták, M.; Hroudová, J. In Vitro Effects of Antipsychotics on Mitochondrial Respiration. *Naunyn-Schmiedeberg's Arch Pharmacol* **2019**, *392*, 1209–1223, doi:10.1007/s00210-019-01665-8.

41. Bolonna, A.A.; Kerwin, R.W. Partial Agonism and Schizophrenia. *The British Journal of Psychiatry* **2005**, *186*, 7–10, doi:10.1192/bjp.186.1.7.

42. McGavin, J.K.; Goa, K.L. Aripiprazole. *Mol Diag Ther* **2002**, *16*, 779–786, doi:10.2165/00023210-200216110-00008.

43. Kneller, L.A.; Zubiaur, P.; Koller, D.; Abad-Santos, F.; Hempel, G. Influence of CYP2D6 Phenotypes on the Pharmacokinetics of Aripiprazole and Dehydro-Aripiprazole Using a Physiologically Based Pharmacokinetic Approach. *Clin Pharmacokinet* **2021**, *60*, 1569–1582, doi:10.1007/s40262-021-01041-x.

44. Aripiprazole. In *LiverTox: Clinical and Research Information on Drug-Induced Liver Injury*; National Institute of Diabetes and Digestive and Kidney Diseases: Bethesda (MD), 2012.

45. Kornischka, J.; Cordes, J. Acute Drug-Induced Hepatitis during Aripiprazole Monotherapy: A Case Report. *J Pharmacovigil* **2016**, *04*, doi:10.4172/2329-6887.1000201.

46. Gao, Y.; Wu, C.; Zhai, X.; Niu, M.; Bai, Z.; Song, H.; Zhao, X.; Wang, J.; Xiao, X. Aripiprazole-Induced Liver Injury: A Spontaneous Reporting Database Study. *Front. Pharmacol.* **2023**, *14*, 1226386, doi:10.3389/fphar.2023.1226386.

47. Hardy, R.E.; Chung, I.; Yu, Y.; Loh, S.H.Y.; Morone, N.; Soleilhavoup, C.; Travaglio, M.; Serreli, R.; Panman, L.; Cain, K.; et al. The Antipsychotic Medications Aripiprazole, Brexpiprazole and Cariprazine Are off-Target Respiratory Chain Complex I Inhibitors. *Biology Direct* **2023**, *18*, 43, doi:10.1186/s13062-023-00375-9.

48. Kramar, B.; Pirc Marolt, T.; Monsalve, M.; Šuput, D.; Milisav, I. Antipsychotic Drug Aripiprazole Protects Liver Cells from Oxidative Stress. *Int J Mol Sci* **2022**, *23*, 8292, doi:10.3390/ijms23158292.

49. Marolt, T.P.; Kramar, B.; Rozman, K.B.; Šuput, D.; Milisav, I. Aripiprazole Reduces Liver Cell Division. *PLOS ONE* **2020**, *15*, e0240754, doi:10.1371/journal.pone.0240754.

50. Kramar, B.; Šuput, D.; Milisav, I. Differential P16 Expression Levels in the Liver, Hepatocytes and Hepatocellular Cell Lines. *PeerJ* **2021**, *9*, e12358, doi:10.7717/peerj.12358.

51. Catalgol, B.; Wendt, B.; Grimm, S.; Breusing, N.; Özer, N.K.; Grune, T. Chromatin Repair after Oxidative Stress: Role of PARP-Mediated Proteasome Activation. *Free Radical Biology and Medicine* **2010**, *48*, 673–680, doi:10.1016/j.freeradbiomed.2009.12.010.

52. Yu, Y.; Yan, Y.; Niu, F.; Wang, Y.; Chen, X.; Su, G.; Liu, Y.; Zhao, X.; Qian, L.; Liu, P.; et al. Ferroptosis: A Cell Death Connecting Oxidative Stress, Inflammation and Cardiovascular Diseases. *Cell Death Discov.* **2021**, *7*, 1–10, doi:10.1038/s41420-021-00579-w.

53. Kale, J.; Osterlund, E.J.; Andrews, D.W. BCL-2 Family Proteins: Changing Partners in the Dance towards Death. *Cell Death Differ* **2018**, *25*, 65–80, doi:10.1038/cdd.2017.186.

54. Verhagen, A.M.; Vaux, D.L. Cell Death Regulation by the Mammalian IAP Antagonist Diablo/Smac.

55. Plotnikov, A.; Zehorai, E.; Procaccia, S.; Seger, R. The MAPK Cascades: Signaling Components, Nuclear Roles and Mechanisms of Nuclear Translocation. *Biochimica et Biophysica Acta (BBA) - Molecular Cell Research* **2011**, *1813*, 1619–1633, doi:10.1016/j.bbamcr.2010.12.012.

56. Han, J.; Wu, J.; Silke, J. An Overview of Mammalian P38 Mitogen-Activated Protein Kinases, Central Regulators of Cell Stress and Receptor Signaling. *F1000Res* **2020**, *9*, F1000 Faculty Rev-653, doi:10.12688/f1000research.22092.1.

57. Barr, R.K.; Bogoyevitch, M.A. The C-Jun N-Terminal Protein Kinase Family of Mitogen-Activated Protein Kinases (JNK MAPKs). *The International Journal of Biochemistry & Cell Biology* **2001**, *33*, 1047–1063, doi:10.1016/S1357-2725(01)00093-0.

58. Runchel, C.; Matsuzawa, A.; Ichijo, H. Mitogen-Activated Protein Kinases in Mammalian Oxidative Stress Responses. *Antioxidants & Redox Signaling* **2011**, *15*, 205–218, doi:10.1089/ars.2010.3733.

59. García-Quintans, N.; Prieto, I.; Sánchez-Ramos, C.; Luque, A.; Arza, E.; Olmos, Y.; Monsalve, M. Regulation of Endothelial Dynamics by PGC-1α Relies on ROS Control of VEGF-A Signaling. *Free Radic. Biol. Med.* **2016**, *93*, 41–51, doi:10.1016/j.freeradbiomed.2016.01.021.

60. Carballo, M.; Conde, M.; El Bekay, R.; Martín-Nieto, J.; Camacho, M.J.; Monteseirín, J.; Conde, J.; Bedoya, F.J.; Sobrino, F. Oxidative Stress Triggers STAT3 Tyrosine Phosphorylation and Nuclear Translocation in Human Lymphocytes. *J Biol Chem* **1999**, *274*, 17580–17586, doi:10.1074/jbc.274.25.17580.

61. Barry, S.P.; Townsend, P.A.; McCormick, J.; Knight, R.A.; Scarabelli, T.M.; Latchman, D.S.; Stephanou, A. STAT3 Deletion Sensitizes Cells to Oxidative Stress. *Biochemical and Biophysical Research Communications* **2009**, *385*, 324–329, doi:10.1016/j.bbrc.2009.05.051.

62. Cheng, X.; Peuckert, C.; Wölfl, S. Essential Role of Mitochondrial Stat3 in p38MAPK Mediated Apoptosis under Oxidative Stress. *Sci Rep* **2017**, *7*, 15388, doi:10.1038/s41598-017-15342-4.

63. Milisav, I.; Moro, F.; Neupert, W.; Brunner, M. Modular Structure of the TIM23 Preprotein Translocase of Mitochondria*. *Journal of Biological Chemistry* **2001**, *276*, 25856–25861, doi:10.1074/jbc.M102132200.

64. Lefaki, M.; Papaevgeniou, N.; Chondrogianni, N. Redox Regulation of Proteasome Function. *Redox Biol* **2017**, *13*, 452–458, doi:10.1016/j.redox.2017.07.005.

65. Meul, T.; Berschneider, K.; Schmitt, S.; Mayr, C.H.; Mattner, L.F.; Schiller, H.B.; Yazgili, A.S.; Wang, X.; Lukas, C.; Schlesser, C.; et al. Mitochondrial Regulation of the 26S Proteasome. *Cell Reports* **2020**, *32*, 108059, doi:10.1016/j.celrep.2020.108059.

66. Collins, G.A.; Goldberg, A.L. The Logic of the 26S Proteasome. *Cell* **2017**, *169*, 792–806, doi:10.1016/j.cell.2017.04.023.

67. Kumar Deshmukh, F.; Yaffe, D.; Olshina, M.A.; Ben-Nissan, G.; Sharon, M. The Contribution of the 20S Proteasome to Proteostasis. *Biomolecules* **2019**, *9*, 190, doi:10.3390/biom9050190.

68. Raynes, R.; Pomatto, L.C.D.; Davies, K.J.A. Degradation of Oxidized Proteins by the Proteasome: Distinguishing between the 20S, 26S, and Immunoproteasome Proteolytic Pathways. *Mol Aspects Med* **2016**, *50*, 41–55, doi:10.1016/j.mam.2016.05.001.

69. Reinheckel, T.; Sitte, N.; Ullrich, O.; Kuckelkorn, U.; Davies, K.J.; Grune, T. Comparative Resistance of the 20S and 26S Proteasome to Oxidative Stress. *Biochem J* **1998**, *335*, 637–642.

70. Ross, J.M.; Olson, L.; Coppotelli, G. Mitochondrial and Ubiquitin Proteasome System Dysfunction in Ageing and Disease: Two Sides of the Same Coin? *Int J Mol Sci* **2015**, *16*, 19458–19476, doi:10.3390/ijms160819458.

71. Du, Z.-X.; Yan, Y.; Zhang, H.-Y.; Liu, B.-Q.; Gao, Y.-Y.; Niu, X.-F.; Meng, X.; Wang, H.-Q. Proteasome Inhibition Induces a P38 MAPK Pathway-Dependent Antiapoptotic Program via Nrf2 in Thyroid Cancer Cells. *J Clin Endocrinol Metab* **2011**, *96*, E763-771, doi:10.1210/jc.2010-2642.

72. Morén, C.; Juárez-Flores, D.L.; Cardellach, F.; Garrabou, G. The Role of Therapeutic Drugs on Acquired Mitochondrial Toxicity. *Current Drug Metabolism* **2016**, *17*, 648–662.

73. Danon, J.J.; Reekie, T.A.; Kassiou, M. Challenges and Opportunities in Central Nervous System Drug Discovery. *TRECHEM* **2019**, *1*, 612–624, doi:10.1016/j.trechm.2019.04.009.

74. Bezerra, T.P.T.; Fabrício, A.I.C.R.; Minervino, A.J.; Santos, R.M. dos Psychoactive Drugs and Metabolic Disorders. *Debates em Psiquiatria* **2023**, *13*, 1–20, doi:10.25118/2763-9037.2023.v13.439.

75. Dimmock, D.P.; Lawlor, M.W. Presentation and Diagnostic Evaluation of Mitochondrial Disease. *Pediatr Clin North Am* **2017**, *64*, 161–171, doi:10.1016/j.pcl.2016.08.011.

76. Tang, X.; Wang, Z.; Hu, S.; Zhou, B. Assessing Drug-Induced Mitochondrial Toxicity in Cardiomyocytes: Implications for Preclinical Cardiac Safety Evaluation. *Pharmaceutics* **2022**, *14*, 1313, doi:10.3390/pharmaceutics14071313.

77. Sokolova, I. Mitochondrial Adaptations to Variable Environments and Their Role in Animals' Stress Tolerance. *Integrative and Comparative Biology* **2018**, *58*, 519–531, doi:10.1093/icb/icy017.

78. Ghonime, M.G.; Shamaa, O.R.; Das, S.; Eldomany, R.A.; Fernandes-Alnemri, T.; Alnemri, E.S.; Gavrilin, M.A.; Wewers, M.D. Inflammasome Priming by Lipopolysaccharide Is Dependent upon ERK Signaling and Proteasome Function. *The Journal of Immunology* **2014**, *192*, 3881–3888, doi:10.4049/jimmunol.1301974.

79. Cirit, M.; Grant, K.G.; Haugh, J.M. Systemic Perturbation of the ERK Signaling Pathway by the Proteasome Inhibitor, MG132. *PLOS ONE* **2012**, *7*, e50975, doi:10.1371/journal.pone.0050975.

80. 8Sandstrom, A.; Mitchell, P.S.; Goers, L.; Mu, E.W.; Lesser, C.F.; Vance, R.E. Functional Degradation: A Mechanism of NLRP1 Inflammasome Activation by Diverse Pathogen Enzymes. *Science* **2019**, *364*, eaau1330, doi:10.1126/science.aau1330.

81. Song, T.; Su, H.; Yin, W.; Wang, L.; Huang, R. Acetylation Modulates LC3 Stability and Cargo Recognition. *FEBS Letters* **2019**, *593*, 414–422, doi:10.1002/1873-3468.13327.

82. Wu, W.-Y.; Kim, H.; Zhang, C.-L.; Meng, X.-L.; Wu, Z.-S. Clinical Significance of Autophagic Protein LC3 Levels and Its Correlation with XIAP Expression in Hepatocellular Carcinoma. *Med Oncol* **2014**, *31*, 108, doi:10.1007/s12032-014-0108-3.

83. Anderson, K.A.; Madsen, A.S.; Olsen, C.A.; Hirschey, M.D. Metabolic Control by Sirtuins and Other Enzymes That Sense NAD+, NADH, or Their Ratio. *Biochim Biophys Acta* **2017**, *1858*, 991–998, doi:10.1016/j.bbabio.2017.09.005.

84. Huang, R.; Xu, Y.; Wan, W.; Shou, X.; Qian, J.; You, Z.; Liu, B.; Chang, C.; Zhou, T.; Lippincott-Schwartz, J.; et al. Deacetylation of Nuclear LC3 Drives Autophagy Initiation under Starvation. *Mol Cell* **2015**, *57*, 456–466, doi:10.1016/j.molcel.2014.12.013.